

# Constructing (multi)functional soil using urban organic and sediment wastes

Received: 19 July 2024

Accepted: 3 September 2025

Published online: 13 October 2025



Lauren Porter<sup>1,2</sup>✉, Franziska B. Bucka<sup>1,3</sup>, Natalie Pérez-Curtidor<sup>4</sup>,  
Monika Egerer<sup>1,2</sup> & Ingrid Kögel-Knabner<sup>1,5</sup>

As urban populations grow, planners must create sustainable, yet multifunctional city spaces. Urban soils are vital for green city initiatives, providing essential ecosystem services. Our research challenges the unsustainable practice of land-take and explores constructing (multi) functional soils from mineral and organic parent materials of the urban waste stream. We stack different qualities of organic amendments in innovative mixtures constructed of upcycled mineral soils from local construction projects to assess their potential in maximizing multiple ecosystem services within a constructed soil. Using key soil health indicators, we identify synergies for the parent material mixtures providing essential functions for urban soils: fertility for urban green, runoff infiltration, stormwater contaminant immobilization and stable carbon accrual. The highest joint multifunctionality is obtained by mixing organic amendments of varying qualities and reactivities. Soil-designing practitioners should be knowledgeable of their city's regional geology, as the effectiveness of amendment mixtures depends on interactions with the geogenic materials.

Urban soils are the foundation of green infrastructure initiatives. However, soils in cities are often compacted, polluted, sealed<sup>1</sup> or otherwise ill suited to provide ecosystem functions<sup>2</sup>. As a solution, suitable soil materials are historically imported from surrounding ecosystems—a practice known as ‘land-take’<sup>3</sup>. However, in recent decades there has been a shift towards a more sustainable practice of re-utilizing surplus sediments and construction wastes<sup>4</sup> as ‘constructed soils’. The re-use of these mineral wastes, accounting for 40% of the annual waste generated in the European Union<sup>5</sup>, supports a circular economy approach within cities to provide soil-based ecosystem services<sup>4</sup>.

In assessing the functionality of such an approach, studies have shown that incorporating mineral structural components such as track ballast, demolition rubble<sup>6–8</sup>, recovered concrete<sup>9</sup> or sorted brick and mortar<sup>10,11</sup> into urban constructed soil mixtures does not acutely diminish nutrient storage and can even improve water cycling in urban green. Moreover, the use of excavated subsoil, the deep soil horizons

displaced during construction projects, may favor soil structural development<sup>12,13</sup>, a central process underpinning many soil functions and services. Yet, organic amendments (OAs) are needed for these mineral parent materials to more closely replicate a fertile topsoil. The use of OAs generated from the urban waste stream—such as biosolids, compost and biochar—can reduce reliance on less sustainable amendments such as peat and chemical fertilizer<sup>14</sup> while still enhancing fertility.

Biochar is a particularly advantageous amendment capable of enhancing soil fertility<sup>15</sup> and potentially replacing benchmark pollutant-retaining materials such as zeolite and activated carbon<sup>16,17</sup>, whose production and use in urban stormwater processing is often energy intensive and costly, contributing to urban carbon emissions<sup>17,18</sup>. As a (by)product of pyrolysis or gasification<sup>19</sup>, biochar can be sustainable alternative, valorizing organic waste while co-producing energy<sup>17,20</sup>. Biochar-amended constructed soils could provide further services in an urban context<sup>21</sup>. Pyrolyzing and redepositing urban waste products,

<sup>1</sup>Chair of Soil Science, School of Life Sciences Weihenstephan, Technical University of Munich, Freising, Germany. <sup>2</sup>Professorship of Urban Productive Ecosystems, School of Life Sciences Weihenstephan, Technical University of Munich, Freising, Germany. <sup>3</sup>Soil Geography and Ecosystem Research, Institute of Physical Geography, Goethe University Frankfurt, Frankfurt am Main, Germany. <sup>4</sup>Chair of Urban Water Systems Engineering, Technical University of Munich, Garching, Germany. <sup>5</sup>Institute for Advanced Study, Technical University of Munich, Garching, Germany. ✉e-mail: [lauren.porter@tum.de](mailto:lauren.porter@tum.de)

such as woody tree clippings, into soils augments soil carbon longevity<sup>22</sup>. This direct form of belowground carbon accrual, combined with any positive influences on urban greening productivity, could represent an offset of 0.3 to 1.2% of annual emissions at the urban scale<sup>21</sup>. However, despite research showing that biochar can improve carbon storage, increase yield, retain pollutants, save water, carry nutrients and reduce acidity, these properties are rarely found all within one source material<sup>15,22</sup>. This discrepancy justifies the incorporation of multiple OAs in urban constructed soils to ensure a broader range of functionalities.

Our research experimentally evaluated the potential of local, circular economy-derived parent materials for constructing multifunctional urban soils. Based in Munich, Germany's most densely populated city, we sourced a regionally typical subsoil—a skeletal sandy clay loam with a carbonate concentration of roughly 50% (Extended Data Table 1a)—from the construction waste of the city's old military base being revitalized as an eco-housing district. Another subsoil from a neighboring urban area served as an additional case study. We aimed to maximize soil properties and functions linked to the socio-environmental benefits of urban green's fertility, runoff infiltration, stormwater contaminant immobilization and carbon accrual by amending the subsoils with combinations of two types of waste-based OA—compost and biochar (Fig. 1). We then compared the OA combinations with a pollutant-adsorption benchmark, granulated activated carbon (GAC)<sup>19</sup> and a low-cost option of only municipal green-waste compost (mGWC).

We evaluated three biochars, two wood-waste (WW) chars of high and low temperature (WW | 850 and WW | 540) and one green-waste (GW) char (GW | 680), sourced from a local provider (Extended Data Table 1b; Carbuna AG, Memmingen, Germany). We tested an OA addition of 4% per mass (~20% by volume), to address economic feasibility and a swift transition of research results to praxis, complying with the upper limit of government mandates for organic matter within constructed soils<sup>23</sup>. Twenty percent by volume has also been suggested as an important threshold in maintaining beneficial hydro-structural functioning while minimizing expensive organic parent material<sup>24</sup>. For each upcycled mineral subsoil, we created nine soil mixtures (Fig. 1)—three controls: (1) subsoil without amendment, (2) a mixture with only mGWC and (3) a mixture incorporating GAC—and six constructed experimental mixtures: (4)–(6) three containing compost and one type of biochar and (7)–(9) three containing compost with two biochars of varying qualities.

Specifically, we asked: does combining OAs of different qualities in waste-based constructed soil enhance soil multifunctionality? We predict the mGWC, and biochar processed at lower pyrolysis temperatures, to substantially increase soil fertility, whereas the (micro) porosity associated with high-temperature wood-waste biochar will augment pollutant retention. Furthermore, although some biochar lend to accrual of stable carbon—containing condensed aromatic carbon compounds similar to activated carbon—these low-reactivity OAs inherently contribute less to organo-mineral associations and, therefore, less to the transition from constructed mixtures to structurally developed soil. We propose that individual biochars are limited in the breadth of their application due to properties unique to their innate feedstock and processing. Using a cascade model, we translate improvements in properties to enhancements in ecosystem functioning and predict that combinations of biochars, along with compost, allows greater synchronization of ecosystem services, which we quantify in a multifunctionality score.

## Results

### Stormwater contaminant immobilization by parent materials

To assess capacity for pollutant removal, we conducted batch adsorption tests with the various parent materials for select heavy metal and organic pollutants in a synthetic stormwater matrix (Fig. 2a,b).

Organic contaminants were represented by the biocides mecoprop and terbutryn—both commonly used in building façade coatings and noted for their high solubility and leaching potential. The removal capacity of the high-temperature wood-waste biochar (WW | 850 BC) was directly comparable to the GAC control, immobilizing 98% of the organic contaminants (Fig. 2a). Combinations of the WW | 850 BC with the medium-temperature green-waste biochar (GW | 680 BC) or the low-temperature wood-waste biochar (WW | 540 BC) showed similar capacities in immobilizing terbutryn ( $98 \pm 0\%$  removal) but reduced capacity for mecoprop ( $89 \pm 3\%$  and  $88 \pm 3\%$  removal, respectively). Alternatively, the use of lower-temperature biochars individually exhibited limited adsorption of the organic contaminants.

The GW | 680 BC achieved high heavy metal removal, immobilizing  $90 \pm 9\%$  of copper and  $83 \pm 8\%$  of zinc (Fig. 2a), surpassing the performance of the GAC control, which averaged  $60 \pm 8\%$  removal across both pollutants. A 1:1 (w/w) dual mixture of WW | 850 and GW | 680 performed similarly well, immobilizing  $> 95\%$  of copper and  $> 70\%$  of zinc. Although WW | 850 BC also demonstrated adequate immobilization of copper ( $84 \pm 5\%$ ) and zinc ( $62 \pm 12\%$ ), removal of both analytes by the WW | 540 BC was decisively poor,  $40 \pm 14\%$  and  $12 \pm 17\%$ , respectively.

Compost alone was able to moderately adsorb heavy metals ( $65 \pm 6\%$  zinc;  $51 \pm 4\%$  copper) but was ineffective in immobilizing organic pollutants ( $31 \pm 9\%$  terbutryn;  $6 \pm 1\%$  mecoprop) (Fig. 2a). Mixtures of compost and individual biochars (1:1 w/w) diminished the immobilization capacity of WW | 850 and GW | 680 on heavy metals by  $7 \pm 12$  and  $4 \pm 13$  percentage points, respectively, while increasing the potential of WW | 540 ( $+ 23 \pm 19\%$  points). Addition of compost decreased WW | 850 and WW | 540 retention of the two organic biocides by an average of  $27 \pm 1$  and  $9 \pm 9$  percentage points, respectively.

Considering an aggregated pollutant removal capacity, GAC ( $79 \pm 22\%$ ), WW | 850 ( $86 \pm 17\%$ ) and the combination of WW | 850 and GW | 680 ( $89 \pm 12\%$ ) resulted in considerably higher total contaminant immobilization than all other OA combinations (Fig. 2b).

The subsoils showed similar capacities to remove heavy metal pollutants, with the medium sand removing  $26 \pm 1\%$  and  $54 \pm 4\%$  of zinc and copper, respectively, and the sandy clay loam removing  $36 \pm 4\%$  and  $69 \pm 5\%$  (Extended Data Table 2). However, immobilization of trace organic compounds was low, with the sandy clay loam removing less than 20% of terbutryn and less than 10% mecoprop, while the medium sand removed effectively zero organic pollutants.

### Boosted fertility parameters in constructed soil mixtures

In mixing the OA combinations with subsoil, we assessed their potential for boosting fertility in constructed soil mixtures. On average, OAs decreased the original bulk densities of the sandy and sandy clay loam mineral materials,  $1.31 (\pm 0.06)$  and  $1.36 (\pm 0.01)$ , respectively, by 9% and 7% (Table 1). This OA-associated drop in bulk density was accompanied by a significant 33% and 12% improvement in the mineral soils' water content at field capacity (Fig. 3). Interestingly, increases in water content associated with OA addition in the sandy subsoil material did not surpass the baseline water content of the sandy clay loam mineral subsoil.

Furthermore, all OA combinations significantly increased total nitrogen content over the initial soil mineral material (Table 1). mGWC and addition of 2% GW | 680 BC displayed the largest influences,  $+ 0.77 \pm 0.07$  and  $+ 0.87 \pm 0.08 \text{ mg g}^{-1}$ , respectively, across the two mineral soils—a roughly 100% increase from the sandy clay loam and 340% and 380% increases for the nutrient-poor sandy soil; significantly higher than the GAC-amended soil mixtures. The pH of the medium sand was neutral ( $7.0 \pm 0.0$ ), whereas the calcareous sandy clay loam ( $\text{CaCO}_3$  content  $51.2 \pm 1.8\%$ ) was mildly alkaline at  $8.3 \pm 0.1$  (Table 1). The organic materials were all alkaline (Fig. 1), ranging from the compost at  $8.1 \pm 0.0$  to GW | 680 BC at  $10.7 \pm 0.2$ , inducing significant increases in pH values over the pure sandy mineral material, and over the 4% mGWC control. OA types showed large differences in improvements to nutrient availability (Table 1). In the sandy clay loam

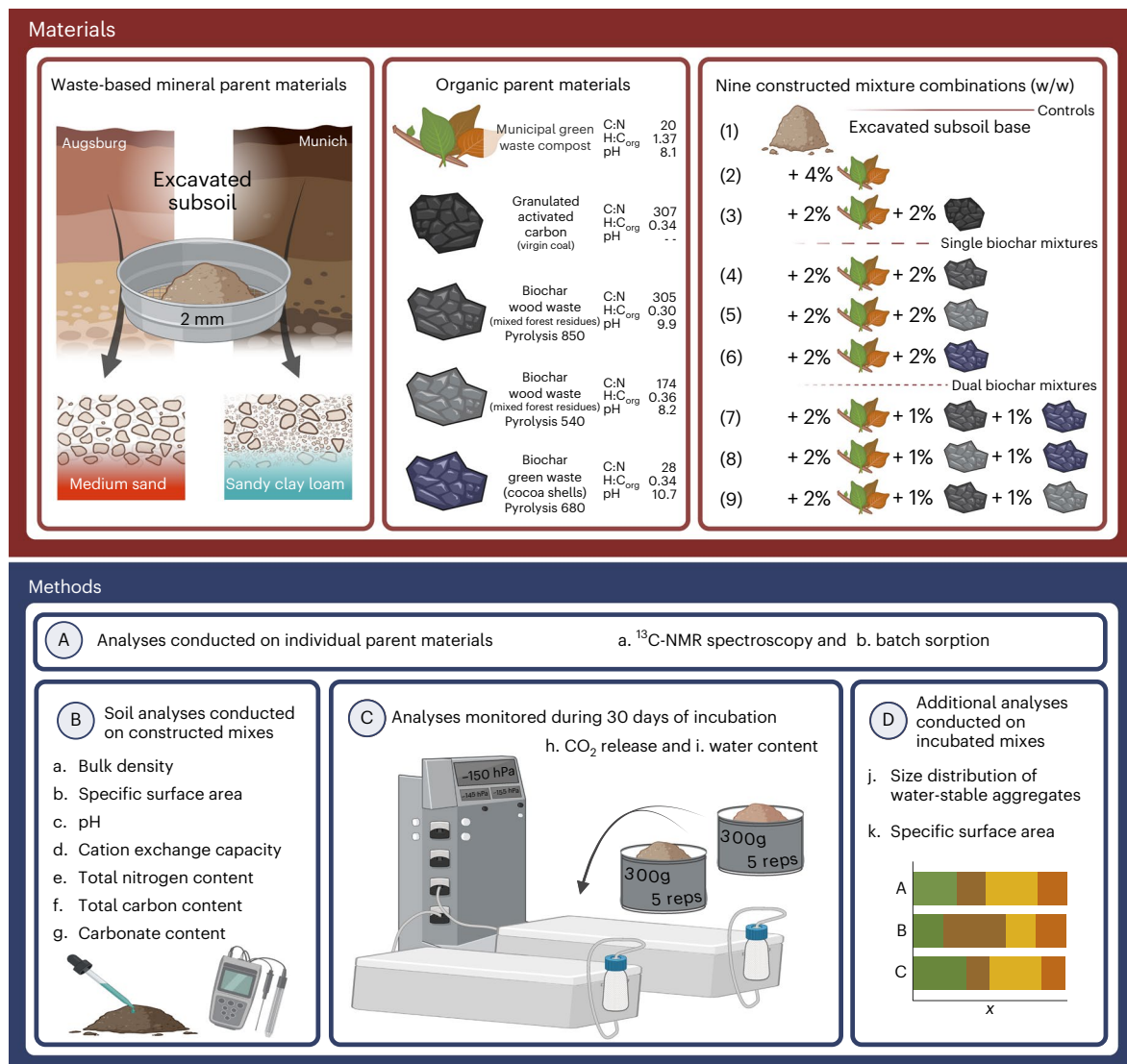


**Fig. 1 | Constructing and assessing soil mixture properties and functions.** The top section in red details the production of the constructed soil mixtures including the processing of the excavated mineral waste, characteristics of the organic amendments and the nine constructed soil mixtures tested in

each subsoil. The bottom section in blue details the analyses conducted on the individual parent materials, conducted on the constructed mixtures, monitored across the 30-day incubation and measured on the harvested, incubated samples. NMR, nuclear magnetic resonance. Figure created using [BioRender.com](https://www.biorender.com).

material, 4% mGWC addition induced a significant 25% increase in total cation exchange capacity (CEC); all other amendments had little to no impact, only sustaining the effective increase from the 2% mGWC within the mixtures. As the initial CEC of the sandy subsoil was quite low, an average of just below  $5 \text{ cmol} \cdot \text{c kg}^{-1}$  soil, the increase induced by even 2% mGWC reflected significant changes in several of the amended mixtures. Consequently, a 4% addition of mGWC afforded an 80% increase in the sandy subsoil's total CEC, significantly higher than all mixtures containing biochar.

### Mineral surface associations and aggregate development across 30 days

We conducted a 30-day incubation on all soil mixtures, per the experimental set-up of Bucka et al. 2021<sup>25</sup>, which documented the rapid transformation of artificial parent materials into structurally stable soil. Although short-term incubations cannot completely predict soil development under field conditions, they can provide an assessment of a soil's pedogenic potential.

Although we observed a small shift towards macro-aggregate formation ((i) in Fig. 4a) in the sandy material, increases in the mean

weight diameter of water-stable soil aggregates ((i) in Fig. 4b)—an indicator for stronger soil structural resistance—were marginal and insignificant. Comparatively in a month's time, we noted an average 41% increase in small macroaggregates ((ii) in Fig. 4a) and a subsequent significantly larger mean weight diameter ((ii) in Fig. 4b) for the sandy clay loam material. Interestingly, in both soil materials, soil structural development in OA mixtures did not significantly differ from that of the excavated subsoil alone (Fig. 4), despite preceding significant increases in microbial respiration across the 30 days of incubation (Table 1).

The available specific mineral surface area (SSA) of the calcareous sandy clay loam and medium sand parent materials were both low at  $8.23 \text{ m}^2 \text{ g}^{-1}$  and  $7.21 \text{ m}^2 \text{ g}^{-1}$ , respectively (Table 1). Dry mixing with 4% mGWC supported early organo-mineral associations in both mineral materials, a calculated  $0.95 \text{ m}^2 \text{ g}^{-1}$  of OM-covered mineral surface in the sandy clay loam and  $0.32 \text{ m}^2 \text{ g}^{-1}$  in the medium sand. Biochar and activated carbon are used as pollutant-immobilizing OAs on behalf of their high porosity and ensuing surface areas<sup>20</sup>. Therefore, we could not rule out that these amendments could both associate with mineral material, covering mineral surfaces, and add surface area. Accordingly, we did not calculate OM-coverage for these mixtures. However, we did

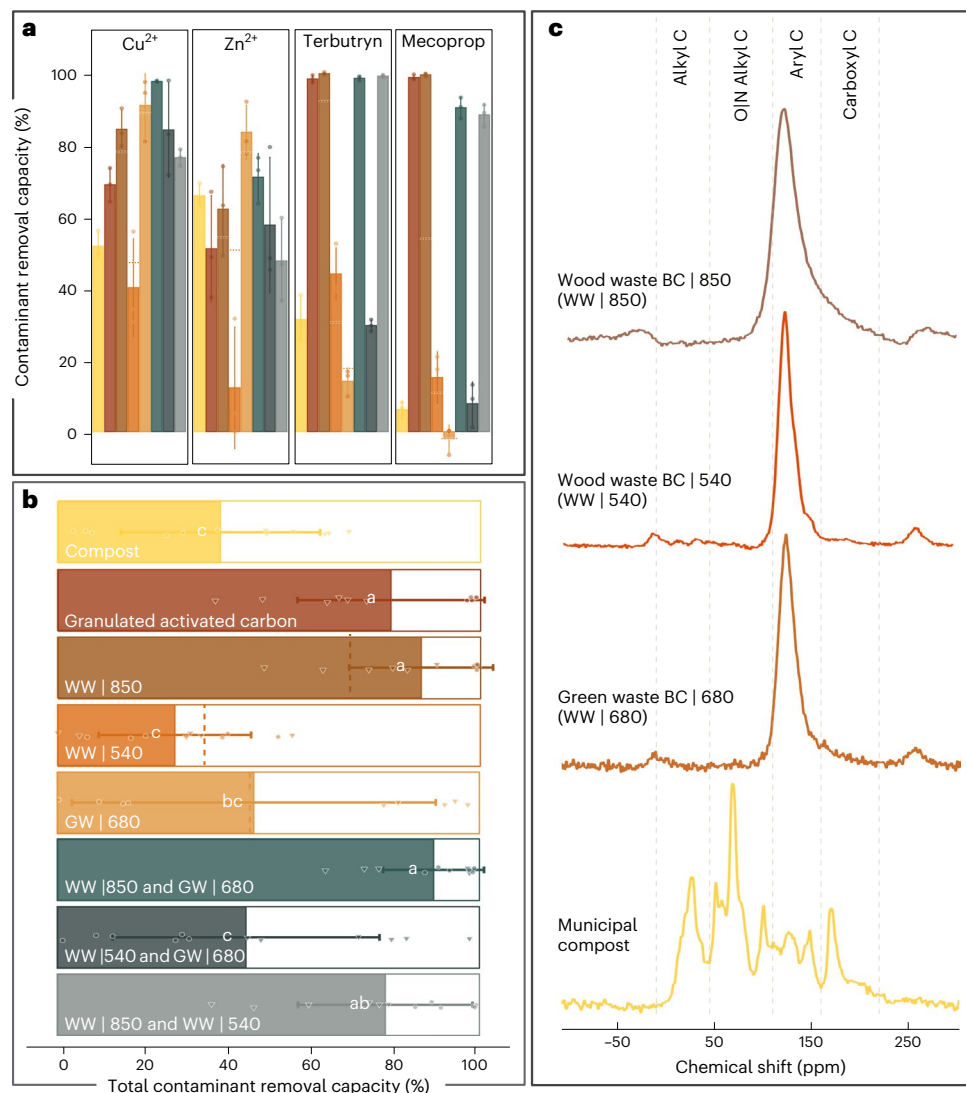


**Fig. 2 | Chemical characteristics and pollutant removal capacity of the OAs.**

**a**, Individual pollutant-retention capacity ( $n = 3$ ) by OAs for the four pollutants tested: heavy metals copper and zinc and biocides mecoprop and terbutryn. Error bars represent the mean  $\pm$  one standard deviation. **b**, The aggregated pollutant-retention capacity ( $n = 12$ ) of the singular and dual biochar treatments, with triangles representing heavy metals and circles representing organic pollutants. Dashed lines indicate non-significant differences between the

singular biochar treatments and mixes containing 1:1 ratio of municipal compost. Error bars represent the mean  $\pm$  one standard deviation. **c**, Results of  $^{13}\text{C}$  NMR spectroscopy ( $n = 1$ ) displaying the relative intensities of the types of carbon bonding at chemical shifts of 0–45 ppm (alkyl C), 45–110 ppm (O/N-alkyl C), 110–160 ppm (aryl C) and 160–220 ppm (carboxyl C) for the biochars and municipal compost. Figure created using [BioRender.com](https://www.biorender.com).

observe soil material-dependent associations of biochar with mineral soil surfaces, with the medium sand showing larger increases in SSA in all dry-mixed biochar-based OA combinations. Addition of 2% GAC resulted in the largest increase in surface area for the mixtures adding approximately  $16 \text{ m}^2 \text{ g}^{-1}$  to each mineral soil, a roughly 210% increase. Whereas the 30-day incubation led to a ubiquitous decline in free mineral surface area of all soil mixtures, OA-amended sandy clay loam mixtures showed strong similarities in reduction to the subsoil mineral material alone (Extended Data Fig. 1a). Alternatively, OA-amended medium sand mixtures showed equal to or greater reduction in available mineral surface area to that of the pure subsoil after incubation (Extended Data Fig. 1b).

### Contributing factors to carbon stabilization

Per definition, amending the mineral soil material with 4% w/w carbonaceous matter led to significant increases in organic carbon that were nearly additive in nature (Table 1 and Extended Data Table 1b). The  $^{13}\text{C}$  nuclear magnetic resonance (NMR) spectra revealed dominantly

aromatic structures (Fig. 2c), indicating the high chemical recalcitrance of the incorporated char materials that increases soil organic carbon residence times. mGWC added significantly less organic carbon per gram amendment to the mixtures (Extended Data Table 1b), moreover, the ratio of aromatic carbon was far lower ( $< 25\%$ ), with easily mineralizable O-alkyl groups representing 40% of the chemical profile (Fig. 2c). Even so, microbial respiration data did not show soil mixtures containing only compost to have higher mineralization rates than those containing biochar or activated carbon (Table 1). Contrarily, the combinations containing 2% GW | 680 BC respired significantly more than the mGWC and GAC controls, holding true for both mineral materials (Table 1). In the sandy soil, this singular biochar mixture also lent to significantly higher cumulative mineralization than either of the 1% w/w dual biochar combination counterparts (Table 1). When auditing our values for carbonate dissolution via normalization to grams of organic carbon, both of our nitrogen-rich mixtures, those containing GW | 680 or 4% GWC, indicated more active microbial communities (Extended Data Fig. 2a).



**Table 1 | Physical, chemical and biological parameters of the constructed soil mixtures underlining different soil functions**

Substrate mixtures	Controls			Single biochar mixtures			Dual biochar mixtures		
	Subsoil	+ 4% mGWC	+ 2% mGWC + 2% GAC	+ 2% mGWC + 2% WW 850	+ 2% mGWC + 2% WW 540	+ 2% mGWC + 2% GW 680	+ 2% mGWC + 1% WW 850 + 1% GW 680	+ 2% mGWC + 1% WW 540 + 1% GW 680	+ 2% mGWC + 1% WW 850 + 1% WW 540
Bulk density (g cm <sup>-3</sup> )									
Medium sand	1.31±0.06	1.26±0.02	1.22±0.01	1.24±0.07	1.20±0.05	1.20±0.07	1.19±0.07 *	1.22±0.03	1.22±0.03
Sandy clay loam	1.36±0.01	1.23±0.04 *	1.24±0.01 *	1.25±0.02	1.23±0.01 *	1.23±0.04 *	1.26±0.03	1.22±0.03	1.24±0.06 *
SSA after dry mixing (m <sup>2</sup> g <sup>-1</sup> )									
Medium sand	7.21±0.12	6.81±0.22	22.84±9.11	9.16±0.32	8.62±0.63	6.71±0.08	7.89±0.08	7.49±0.02	8.30±0.65
Sandy clay loam	8.23±0.11	7.26±0.12	25.31±3.05	8.86±0.43	7.34±0.56	6.76±0.31	8.07±0.53	7.53±0.35	7.88±0.74
pH									
Medium sand	7.00±0.02	7.16±0.07	7.45±0.05 *	7.39±0.02 *	7.69±0.15 <sup>Δ</sup>	8.22±0.09 <sup>Δ</sup>	7.30±0.38 *	7.67±0.03 <sup>Δ</sup>	7.36±0.11 *
Sandy clay loam	8.30±0.10	8.31±0.01	8.52±0.01	8.45±0.05	8.44±0.03	8.94±0.05 <sup>Δ</sup>	8.75±0.01 <sup>Δ</sup>	8.68±0.03 <sup>Δ</sup>	8.45±0.02
CEC (cmol·c kg <sup>-1</sup> )									
Medium sand	4.75±0.89	8.54±1.61 *	6.23±0.72	6.63±0.81 <sup>Δ</sup>	6.59±0.87 <sup>Δ</sup>	6.52±0.46 <sup>Δ</sup>	6.12±0.47 <sup>Δ</sup>	6.33±0.61	5.82±1.11 <sup>Δ</sup>
Sandy clay loam	9.320±1.57	11.74±0.65 *	10.25±0.48	10.12±0.51	10.01±0.25 <sup>Δ</sup>	10.47±0.55	10.21±0.57	10.24±0.52	10.21±0.08
TN (mg g <sup>-1</sup> )									
Medium sand	0.24±0.01	0.98±0.17 *	0.61±0.11 *	0.90±0.20 <sup>Δ</sup>	0.86±0.27 <sup>Δ</sup>	1.22±0.18 <sup>Δ</sup>	0.66±0.10 <sup>Δ</sup>	1.00±0.23 *	0.65±0.10 <sup>Δ</sup>
Sandy clay loam	0.79±0.04	1.58±0.13 *	1.18±0.04 *	1.16±0.07 <sup>Δ</sup>	1.23±0.09 <sup>Δ</sup>	1.55±0.16 <sup>Δ</sup>	1.28±0.05 <sup>Δ</sup>	1.39±0.10 *	1.24±0.08 <sup>Δ</sup>
C to N ratio									
Medium sand	10.2±0.6	15.7±0.4 *	40.9±7.7 *	36.6±2.7 <sup>Δ</sup>	35.6±3.0 <sup>Δ</sup>	20.2±0.8 <sup>Δ</sup>	24.3±1 <sup>Δ</sup>	28.1±2.8 <sup>Δ</sup>	36.5±2.5 <sup>Δ</sup>
Sandy clay loam	10.2±2.7	17.1±1 *	32.8±3.6 *	26.5±2.5 <sup>Δ</sup>	27.1±2.1 <sup>Δ</sup>	16.4±0.5 <sup>Δ</sup>	20.5±1.2 <sup>Δ</sup>	22.7±3.4 <sup>Δ</sup>	26.1±3.4 <sup>Δ</sup>
TOC (mg g <sup>-1</sup> )									
Medium sand	1.44±0.15	14.66±3.32 *	24.98±8.28 *	32.77±6.5 <sup>Δ</sup>	31.25±12.74 <sup>Δ</sup>	24.34±4.81 *	15.86±3.13 *	27.66±9.23 <sup>Δ</sup>	24.04±5.33 *
Sandy clay loam	9.94±0.73	26.19±3.12 *	38.79±2.25 *	30.99±4.41 *	33.88±2.57 *	29.96±4.06 <sup>Δ</sup>	27.04±1.85 <sup>Δ</sup>	35.02±4.47 *	34.46±3.23 *
CaCO <sub>3</sub> (mg g <sup>-1</sup> )									
Medium sand	0	ng	ng	ng	ng	ng	ng	ng	ng
Sandy clay loam	512±18	447±19	465±20	451±24	470±22	500±14	481±9	460±36	483±34
Respired mgC-CO <sub>2</sub> g <sup>-1</sup> soil									
Medium sand	0.10±0.01	0.27±0.03 *	0.28±0.04 *	0.29±0.02 *	0.27±0.03 *	0.38±0.03 <sup>Δ</sup>	0.32±0.02 *	0.32±0.01 <sup>Δ</sup>	0.30±0.02 *
Sandy clay loam	0.31±0.02	0.39±0.01 *	0.38±0.02 *	0.36±0.01 *	0.39±0.02 *	0.44±0.02 <sup>Δ</sup>	0.40±0.02 *	0.42±0.01 *	0.40±0.02 *

Values are represented as means ± one standard deviation. Abbreviations: mGWC, municipal green-waste compost; GAC, granulated activated carbon; WW|850, high-temperature wood-waste biochar; WW|540, low-temperature wood-waste biochar; GW|680, green-waste biochar; CEC, cation exchange capacity; TN, total nitrogen; TOC, total organic carbon. Percentages indicate mass contribution of high carbon organic amendments to the mixtures. Fig. 1 provides further clarifications. All parameters contain *n*=5 replicates, with the exception of bulk density (sandy clay loam, *n*=3; medium sand, *n*=4) and specific surface area (SSA) after dry mixing (*n*=2). Total nitrogen, organic carbon and calcium carbonate contents are representative of dry-mixed soils, whereas respired carbon is accumulated total across 30 days of incubation. Differences between treatments were analyzed using one-way ANOVA, with targeted post-hoc orthogonal contrasts restricted to predefined comparisons. \* Significant difference found between the property of the subsoil and amended mixture Δ Significant difference found between the property of the green-waste compost control and a biochar-amended mixture † Significant difference found between the property of the granulated activated carbon control and a biochar-amended mixture § Significant difference found between the property of a singular biochar mixture compared to the related dual biochar mixtures

## Discussion

Our work shows the ecological value of amending urban mineral wastes with OAs of different qualities, promoting a circular soil economy<sup>4</sup>. Ecological value is derived from synergizing an increasing number of soil services, which we calculate using a simple standardized indicator- and average-based multifunctionality score (0 to 1) for our constructed soil mixtures amended with mGWC and biochar (Fig. 5; Supplementary

Section A). We find that while addition of mGWC alone has limited multifunctionality (0.48 ± 0.05), dual biochar mixtures containing high-temperature wood-waste biochar (WW|850 BC) achieve a multifunctionality balance (0.81 ± 0.03) equivalent to soil mixtures containing GAC (0.80 ± 0.06). However, the singular WW|850 BC mixture holds the highest multifunctionality score (0.88 ± 0.05), challenging our hypothesis that biochars of different qualities are needed to enhance

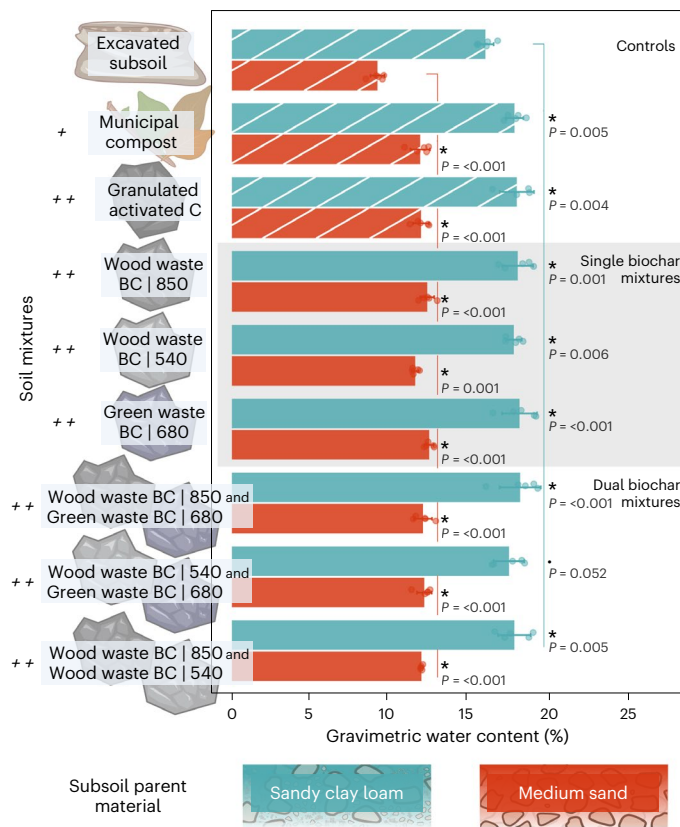


**Fig. 3 | Gravimetric water content at field capacity.** ( $n = 5$ ). Fig. 1 provides soil mixture clarifications. Asterisk (\*) indicates significant differences from the subsoil control that were analyzed using one-way ANOVA, with targeted post-hoc orthogonal contrasts restricted to predefined comparisons. Error bars represent the mean  $\pm$  one standard deviation. Figure created using [BioRender.com](https://www.biorender.com).

multifunctionality. Nevertheless, our results make evident that biochar and compost control different soil functions.

The low N contents in our mixtures are comparable to other, unsealed urban soils<sup>26,27</sup> and to B or C horizons of local grasslands<sup>28</sup>, with CECs similar to other waste-based constructed soils<sup>6</sup>. Of the OAs tested, only mGWC contributed significant amounts of primary and secondary macro-nutrients (Table 1; Extended Data Table 3) to the soil mixtures, advocating for its inclusion as the base OA in otherwise infertile mineral constructions. Biosolids, a waste-based OA not explored in this study, also offer a fast-releasing supply of nutrients, particularly phosphorus<sup>14</sup>. However use of biosolids on soils in Germany, and probably other European countries to follow, is being phased out, making composting pathways a safer investment for municipalities. Adequate water and air supply are also important features for urban greening<sup>29</sup>. Despite differences in OA type, particle size distribution and pyrolysis production temperatures (Extended Data Table 1b), we found no significant differences between the bulk densities and water-holding capacities of the amended soils (Table 1 and Fig. 3)<sup>15,30</sup>. This supports the universality of OAs' positive effects on plant-available water retention<sup>24,31</sup> and bulk density, suggesting practitioner choice in OA combinations can be made based on other parameters. Function scoring, weighed evenly between increases sustained in CEC, N content and water content at field capacity, revealed mixtures with 4% mGWC ( $0.91 \pm 0.16$ ) and 2% green-waste biochar (GW | 680 BC;  $0.75 \pm 0.13$ ) added the most to soil fertility.

In our scoring the function of aggregated pollutant immobilization capacity, all biochar mixtures containing WW | 850 achieved scores equal to or greater than the GAC control ( $0.89 \pm 0.04$ ; Supplementary Section A and Fig. 2b). The capacity of GAC, virgin coal

that is physically or chemically 'activated' to increase its porosity, to immobilize pollutants is often attributed to its high SSA—particularly pertaining to organic pollutants<sup>20</sup>. Accordingly, the GAC-amended mixtures depicted over a 200% increase in SSA (Table 1). However, similar organic pollutant immobilization by biochars were not accompanied by the same drastic increases in amended soil mixtures SSA. We hypothesize the European Biochar Certification-certified measure for SSA, N<sub>2</sub> gas diffusion, may underestimate biochar surface area by up to two orders of magnitude<sup>32</sup>, and this unmeasured range of micropores, often associated with high-temperature biochars, could contribute to the highly effective organic pollutant-retention capacity of WW | 850. Furthermore, the presence of high aromaticity, evidenced by the aryl carbon content in the <sup>13</sup>C NMR spectra, could instigate hydrophobic interactions offering an additional pollutant-stabilizing mechanism<sup>33</sup>. These phenyl structures, together with surface functional groups containing nitrogen<sup>34</sup>, provide electrostatic attraction<sup>33</sup> with the potential to bind the heavy metal cations, leading to stronger retention by the two higher temperature biochars. We also acknowledge the highly alkaline pH values of the OAs, particularly the green-waste-based biochar (Extended Data Table 1b), which suggest further stabilization of heavy metals via precipitation as hydroxides or carbonates<sup>33</sup>. Of note, the pH of an evolving soil system should be taken into consideration when relying on precipitation as an immobilization mechanism, as acidifying mineral material would hinder long-term retention of some heavy metals. Furthermore, mGWC—a nutrient-rich compound—and combinations thereof, displayed weaker pollutant immobilization capacities, particularly of organic pollutants. This indicates a trade-off in pollutant retention when augmenting mixtures for fertility, as contaminant sorption is defined by the available binding sites in a soil, sites for which nutrients and pollutants may directly compete.

Stable soil structure makes it possible to use soils, rather than just sand or gravel, in green infrastructure systems intended for infiltration and drainage, with the coinciding benefit of greater carbon storage potential<sup>35</sup>. However, the development of a stable soil structure, at least via natural pedogenic processes, takes years to decades, directly conflicting with timeframes of urban initiatives where time from installation of a constructed soil to the use of a green space may occur in months, if not weeks. Considering this limitation, we tested the feasibility of rapid (30 days) water-stable aggregate formation, encouraged by successes in both artificial and constructed soils<sup>12,25,36</sup>. Within our 30-day experiment, we did not find water-stable structural development in the sandy soil but did observe greater mean weight diameter of aggregates in the sandy clay loam soil mixtures. Interestingly, our results present no significant differences between the excavated subsoils and the amended treatments (Fig. 4), downplaying the role of organic matter-mediated structural formation in the first 30 days. Our results imply that any rapid increase in aggregation is contingent on the subsoil parent material rather than the introduction of organic matter.

Furthermore, we observed a large amount of biochar floating after our wet-sieving treatment, suggesting a low bond strength between the biochar and mineral fraction<sup>37</sup>. For biochar, nucleation of structural aggregates, like many other functionalities, is dependent on surface chemistry. Results from our <sup>13</sup>C NMR spectroscopy (Fig. 2), in combination with the H to C<sub>org</sub> ratio (Fig. 1), suggest the absence of reactive functional groups. Although our findings are in line with studies that illustrate biochar application to be neutral or even antagonistic to aggregate formation<sup>36,38–42</sup>, other studies have demonstrated biochar's ability to instigate soil particle agglomeration<sup>39,40,43,44</sup>. In reviewing the literature reporting biochar-instigated aggregation within short timeframes, we found biases in biochar chemical composition, with many studies either using chars processed at lower pyrolysis temperatures<sup>39,44</sup> or char in mixtures with more labile material<sup>40,43</sup>. Therein, we conclude that municipal compost, granulated activated carbon and both green-waste and wood-waste biochars (>500 °C) are all unfit to initialize rapid structural formation in these soil materials.

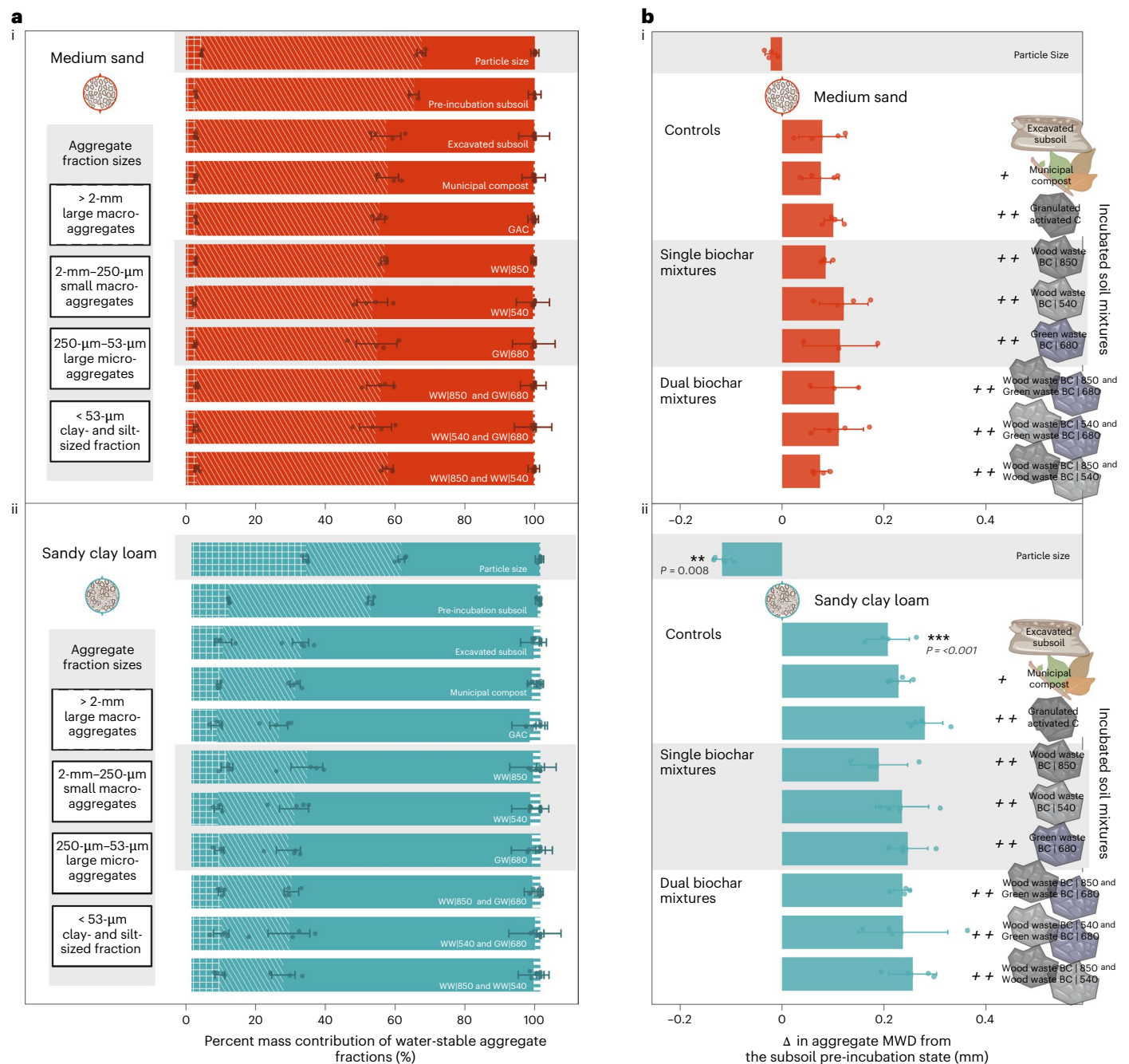


**Fig. 4 | Soil structural development. a**, Development of water-stable aggregate size distribution, represented by four size fractions, as seen in the primary particle size of the subsoil without aggregates, the excavated subsoil pre-incubation ( $n = 3$ ) and the development of the subsoil and soil mixtures after 30 days of incubation ( $n = 4$ ) **b**, Changes in water-stable aggregate mean weight diameter (MWD) from the pre-incubation time point ( $n = 4$ ); asterisks indicate

significant differences in mean weight diameter from the excavated subsoil before incubation investigated using one-way ANOVA, with targeted post-hoc orthogonal contrasts restricted to predefined comparisons. Fig. 1 provides soil mixture clarifications. Error bars represent the mean  $\pm$  one standard deviation. Figure created using BioRender.com.

We recommend further research on constructing multifunctional soils for urban green initiatives focused on the intersection of infiltration, drainage and carbon cycling to investigate more intensive mixing approaches using labile, intermediate and recalcitrant organic parent materials to help stimulate both a rapid and sustainable development of soil structure.

Although biochar lends little to the protective process of stable aggregate occlusion, char's complexity and the infrequent occurrence of its chemical form<sup>45</sup> heightens microbial investment for mineralization, increasing its longevity in soils. Recent opinions suggest

amending with this type of organic matter is the preferred approach for increasing C stocks in soils with a low proportion of reactive minerals<sup>46</sup>, such as our subsoil-based mixtures. Though our function scoring excludes the function of infiltration due to no significant differences in structural development between amended soils, we include the service of stable carbon accrual; here the mixtures with 2% WW | 850 BC ( $1.00 \pm 0.01$ ) and GAC ( $0.95 \pm 0.11$ ) demonstrate the highest potential (Supplementary Section A).

The results of our study emphasize the importance of different geogenic qualities on ecosystem service potential in constructed urban



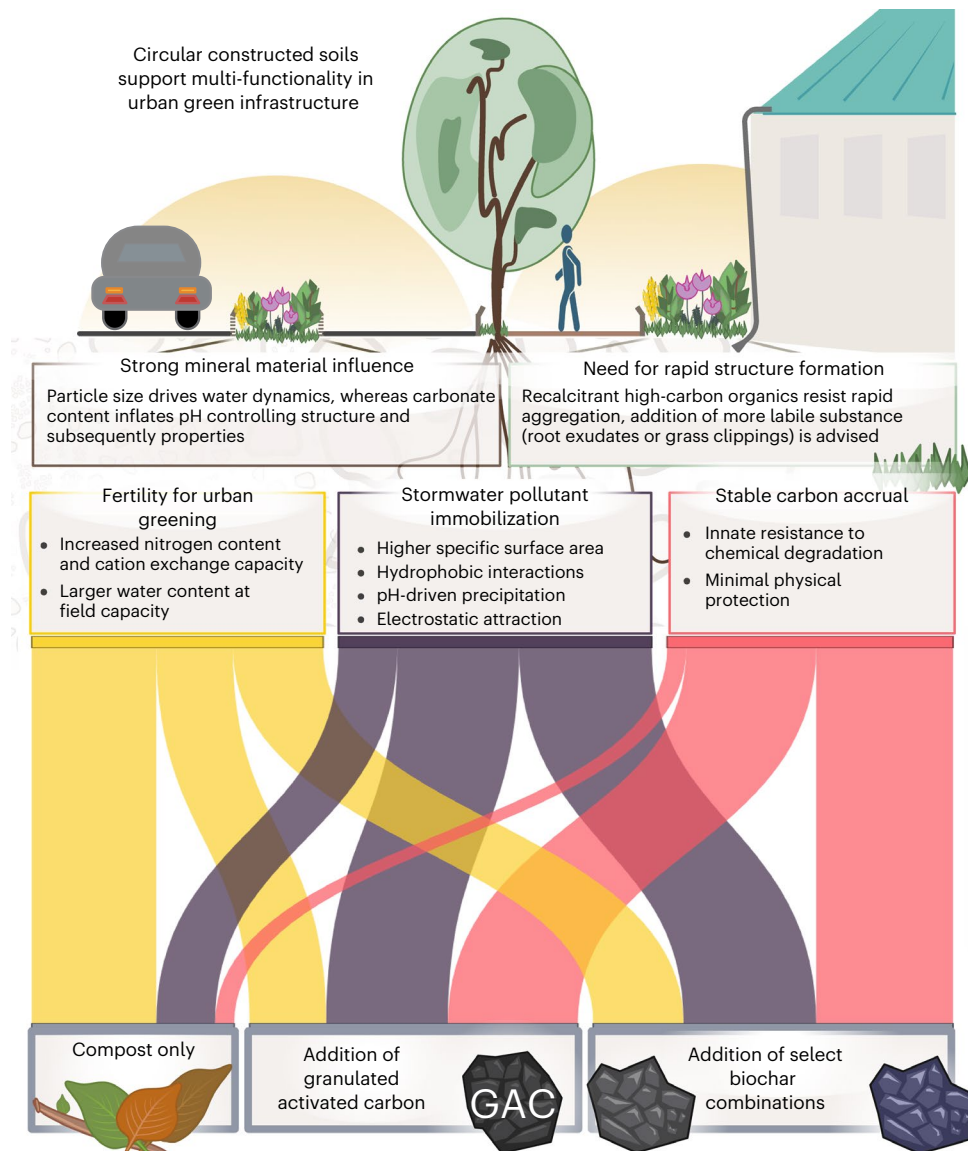


**Fig. 5 | Conversion of sediment construction wastes to multifunctional soil mixtures via addition of organic amendments.** Limitations and synchronization of ecosystem services. Figure created using [BioRender.com](https://www.biorender.com).

mixtures and subsequent soil. Although both mineral subsoils failed to retain organic pollutants, they exhibited natural attenuation of heavy metals (Extended Data Table 2). This effect was more pronounced in the sandy clay loam, probably due to its higher clay and carbonate content, which enhanced its capacity for heavy metal immobilization<sup>47</sup>. A high carbonate content also contributes to a more alkaline soil environment, which in turn influences both carbon and nutrient storage dynamics<sup>48</sup>. Furthermore, although our study lacked amendment-initiated water-stable aggregate development, we hypothesize the characteristic larger carbonate<sup>49</sup> and clay fractions<sup>50</sup> of the sandy clay loam parent material to induce abiotic gluing within the 30-day incubation, increasing the soil structural stability (Fig. 4). Geogenic properties also entail certain trade-offs. The calcareous cementing that allows for rapid structural formation may also diminish root space, while the increase in pH associated with higher carbonate content may limit nutrient availability for urban green. The influence of particle size is also clear, exemplified in the baseline difference in the water content of the excavated subsoils at field capacity (Fig. 3), as additions of reasonable quantities of OAs to sandy soil material could not overcome the inherent capacity of a finer soil material. These results raise the importance of knowledgeably

constructing functional soil mixtures, choosing OAs to balance the weaknesses of the available mineral material.

## Conclusion

Our findings highlight the functional performance of amended, circular-economy-based soil mixtures. Whereas all tested amendments improved soil physical and chemical properties of construction-derived subsoil mineral materials, select combinations of municipal green-waste compost and biochar outperformed both compost alone and mixtures containing granulated activated carbon, a common standard for pollutant immobilization. Using a cascade model, we translated these improvements in soil properties to quantitative scores for soil ecosystem services, comparing the functions of fertility for urban greening, stormwater contaminant immobilization and stable carbon accrual.

Nitrogen content and cation exchange capacity, two soil health indicators supporting plant fertility, were almost exclusively supplied by additions of compost, supporting its role as the base organic amendment in these mixtures. Despite its central role in fertility, we found a trade-off in compost's pollutant immobilization functionality score. Here select biochar combinations exhibited high over overall retention



of both organic and heavy metal pollutants, scoring higher in this functionality than granulated activated carbon. Although our scoring system showed the accrual of chemically stable carbon associated with the high-temperature wood-waste biochar mixtures to be equivalent to that of the activated carbon, none of the tested organic amendments initiated rapid water-stable aggregate formation that could both enhance hydraulic conductivity and act as an intermediate carbon storage pool. We affirm here the need for further mixing of organic parent material of different qualities—including more labile compounds as nuclear particulate organic matter to prompt aggregation and therefore further increase the multifunctionality of the mixture.

Overall, the multifunctionality score of mixtures contain compost alone was low, whereas biochar mixtures containing high-temperature wood-waste biochar achieved an equal or higher multifunctionality balance than those containing granulated activated carbon. Urban migration and densification place higher demands on city spaces, making it increasingly important to enhance the value of our green spaces by adding additional functions and benefits. Our findings emphasize that the highest joint multifunctionality score is obtained by mixing amendments of varying qualities and reactivities, though the necessity of an amendment is function dependent. We emphasize that practitioners should be knowledgeable of their city's geological background, ecosystem service enhancement is dependent on the educated choice in amendments and their interactions with geogenically controlled variables.

## Methods

Two subsoil materials of the study were provided by Bodeninstitut Prögl and Andreas Thaler, representing typical 'waste soils' excavated during construction projects. Sampled from the glaciofluvial gravel terrace deposits of the Alps, commonly referred to as the Munich gravel plain<sup>51</sup>, the first soil material is a transition horizon 20- to 40-cm thick between the topsoil and pure gravel, locally referred to as a 'Rotlage'<sup>52</sup>. This skeletal sandy loam material with a high carbonate concentration (> 50%) is a Cw(T) horizon of a calcaric Regosol. Found on the Langweider high terrace along the river Lech and characterized by sandy loess<sup>53</sup>, the Augsburg soil material is a Bw horizon from a cambic Arenosol. The particle size distribution (Extended Data Table 1a) of these bulk soils naturally resist compaction and accommodate mandated infiltration rates set for urban green spaces intended for decentralized infiltration (DWA 2020). However, to conduct pertinent soil analyses, we investigate the ecological functions of a homogenized, active soil fraction (< 2 mm) (Fig. 1). The extent to which the bulk soils would be sieved is project dependent, but we conjecture that fertility and pollutant retention measured for the active soil fraction will be proportional to the ratio of the active to coarse fraction within a soil material, as often measured with carbon stocks<sup>54</sup>.

Biochars were chosen on the basis of availability from the local supplier; preference was given to feedstocks that were not manure- and sludge-based chars due to the lower potential of contamination and nutrient leaching<sup>55</sup> and to biochars endorsed by the European Biochar Certification.

## Analyses conducted on individual components

We determined particle size distribution of the mineral soils in duplicates, sieving to 2 mm then removing organic matter and carbonates by 30% H<sub>2</sub>O<sub>2</sub> and 1 M HCl, respectively (Extended Data Table 1a). Coarse content data (> 2 mm) were obtained from testing agency factsheets. Samples were rotated overnight (> 16 h) with 0.025 M Na-Pyrophosphat. The sandy fractions (> 63 µm) were wet sieved, whereas silt and clay fractions were freeze dried and determined via X Ray sedimentation (Sedigraph III PLUS, Micromeritics). Biochar particle size distributions were provided to 0.33 mm by the company, however compost and granulated activated carbon were manually dry sieved (*n* = 2) to 0.5 mm (Extended Data Table 1b).

The chemical composition of the OAs was characterized using solid-state <sup>13</sup>C NMR spectroscopy (*n* = 1; Bruker Biospin DSX 200 NMR spectrometer), where samples were spun in a magic angle spinning probe<sup>56</sup> at a rotation speed of 6.8 kHz with an acquisition time of 0.4 ms. The obtained spectra were integrated according to four major chemical shift regions: 0–45 ppm (alkyl C), 45–110 ppm (O/N-alkyl C), 110–160 (aryl-C) and 160–220 ppm (carboxyl-C)<sup>57</sup>, with the alkyl C:O alkyl C ratio (–10–45/45–110 ppm) further computed to describe the degree of aliphaticity<sup>58</sup>. In measuring the high-temperature wood-waste biochar and granulated activated carbon, we experienced difficulties in obtaining a clean spectra, probably due to the high electrical conductivity that correlates with the stacking of aromatic sheets<sup>59</sup>. The H to C<sub>org</sub> ratio for the organic amendments was calculated from an elemental analysis conducted by the TUM Catalysis Research Center in Garching, Germany (HEKATech EURO-EA).

We employed batch adsorption experiments (*n* = 3) using a synthetic stormwater matrix representing mixed urban runoff (composition as reported in Spahr et al. 2022<sup>60</sup>) to assess the adsorption performance of the OAs and soil materials (Supplementary Section B). Mixtures of biochar (1:1) and mixtures of biochar and compost (1:1) were also tested. The adsorption performance of the biochars and the mixtures were compared with that of granular activated carbon. Soil and compost were also tested to evaluate their potential for enhancing the removal of both heavy metals and biocides. The testing vessels containing 0.5 g l<sup>−1</sup> of adsorbent were spiked after a 24-hour pre-equilibration time to achieve a target concentration of 100 µg l<sup>−1</sup> of the heavy metals copper and zinc and the biocides mecoprop and terbutryn. Three vessels of synthetic stormwater, spiked with pollutants but without adsorbents, were tested as control samples. The concentration of heavy metals and biocides after five days of contact with the adsorbents was measured through flame atomic absorption spectrometry (Varian Spectrometer AA-240FS). The limit of quantification (LOQ) was 5.0 µg l<sup>−1</sup> for copper and 20.0 µg l<sup>−1</sup> for zinc. The biocide concentration was determined through liquid chromatography coupled to mass spectrometry. The LOQ for all biocides was 25 ng l<sup>−1</sup>.

## Analyses conducted on dry-mixed soil combinations

Figure 1 lists the analyses conducted on the dry-mixed, homogenized soil combinations. Bulk density (g cm<sup>−3</sup>) was measured with three replicates by loading approximately 100 g soil into 100 cm<sup>3</sup> soil cores. Each core was tapped three times to allow settling of soil but not to use over-head pressure for compaction, before being saturated overnight and placed on a suction plate (EcoTech Umwelt-Messsysteme) to determine volume at field capacity, here a water tension of −15 kPa. Mixtures were then dried at 105 °C to determine the corresponding soil weight. Specific surface area (SSA) of the soil mixtures was measured with two replicates via multipoint N<sub>2</sub>-BET<sup>61</sup> (m<sup>2</sup> g<sup>−1</sup>; AUTOSORB-1, Quantachrome Instruments) using approximately 2–3 g of air-dried material outgassed with He (> 14 h at 40 °C under vacuum).

Calcium carbonate content of mixtures and individual components were quantified using a calcimeter (Eijkelkamp), and inorganic carbon contents were calculated as 12% of the measured calcium carbonate per the International Organization for Standardization formula ISO 10693 (*n* = 5; mg g<sup>−1</sup>). Total carbon, organic carbon and total nitrogen contents were then measured via dry combustion by a CN analyzer (HEKATech) (*n* = 5; mg g<sup>−1</sup>). Organic carbon contents were obtained by adding sufficient HCl to destroy the inorganic carbon within the samples before combustion.

The nitrogen values, particularly of the unamended subsoil, approach the detection limits of the instrument, rendering significant differences in computed nitrogen balances ineffectual. However it should be noted, in an additive evaluation of our parent materials, our sandy substrate was amended with 2% WW | 850 BC and that with 2% GW | 680 BC (+ 0.30 and + 0.21 mg g<sup>−1</sup>, respectively) and the sandy clay loam with only compost (+0.20 mg g<sup>−1</sup>) to contain marginally

more nitrogen than expected from the individual components (Supplementary Section C). In budgeting for the maximum total N in our system after incubation, including small nutritional inputs to not limit microbial growth, we observed compost ( $35 \pm 19\%$  medium sand,  $19 \pm 8\%$  sandy clay loam) and singular biochar mixtures, most notably WW | 850 ( $44 \pm 22\%$ ,  $13 \pm 6\%$ ), to contain less N than theorized; whereas the combination of WW | 850 and GW | 680 BC maintained theoretical levels ( $4 \pm 19\%$ ,  $4 \pm 7\%$ ).

The pH value of the mineral material and soil mixtures were conducted with a pH Meter (Mettler-Toledo SevenEasy S20;  $n = 5$ ) in a 1:2.5 soil to deionised water ratio, whereas the individual OAs were measured at more diluted ratios of 1:5 and 1:10 for compost and biochar, respectively. Due to immediate liquid–solid phase separation the pH value of the granulated activated carbon as an individual OA was not measured. Samples were shaken at 100 r.p.m. for 1 h, before allowing to settle for another hour before analysis. Total cation exchange capacity and effective cation exchange capacity (macro-nutrient ions  $K^+$ ,  $Na^+$ ,  $Mg^{2+}$ ,  $Ca^{2+}$ ) of the soil mixtures were obtained following the German Handbook for Forestry Soil Analysis (König et al. 2005) ( $n = 5$ ;  $cmol \cdot c \cdot kg^{-1}$ ). In short, 2.5 g of each sample was percolated first with a  $BaCl_2$  solution, followed by  $MgCl_2$ . Both effluents were collected and the cation ion sum (Ca, Mg, K and Na) and the total Ba ion release were measured and compared via inductively coupled plasma (ICP) analysis (Vista-PRO CCD Simultaneous ICP-OES, Varian Inc.).

### Incubation experimental set-up and concurrent analyses

The set-up of the incubation experiment followed the procedure of Bucka et al. 2019<sup>62</sup>, shortly: 300 g of an air-dried soil mixture homogenized by repeated mixing was filled into a microcosm and placed onto a suction plate (polyamide membrane, pore size 0.45  $\mu m$ , EcoTech Umwelt-Messsysteme) at a water tension of  $-15$  kPa (corresponding to a pF value of 2.2, approximate field capacity of loamy sands) in a closed hydraulic system.

During the first three days of the experiment, 30 ml of a 1:10 diluted Hoagland's solution (pH 5.5, Hoagland's No 2 basal salt mixture, Sigma-Aldrich) was administered per day to ensure all pores were filled and that the samples could then equilibrate to  $-15$  kPa. Thereafter, 10 ml were administered after each respiration measurement (every 48–72 h) to counteract evaporation, leading to a total input of 368 mg of nutrient powder per microcosm. Gravimetric water content was monitored by weight throughout the incubation and used as a single indicator of plant-available water content due to the high correlation between increases in water content at field capacity and plant-available water content with soil organic matter (SOM) addition<sup>63</sup>. Five replicates of each soil mixture were incubated for a total of 30 days in the dark at a constant temperature of 20 °C (Fig. 1, box 4; as an exception, one replicate of the sandy clay loam containing granulated activated carbon was lost during handling).

$CO_2$  release of the microcosms was measured every 48 to 72 h by placing the samples into air-tight containers for approximately 5 h, capturing the  $CO_2$  released in 15 ml of 0.1 M NaOH solution. Afterwards, 2 ml of  $BaCl_2$  were added to stop the reaction from reversing before the NaOH solution was titrated to pH 8.3 (Mettler-Toledo), according to Bimüller et al. 2014<sup>64</sup> and Luxhøj et al. 2006<sup>65</sup>. Respiration was extrapolated for days during which respired  $CO_2$  was not measured (Extended Data Fig. 2b), allowing the overall  $CO_2$ -C release to be determined. A cross-soil material comparison of the cumulative  $CO_2$  respiration values normalized to grams of organic carbon is used as evidence for the minimal to non-existent transformation of the carbonates present in the calcareous sandy clay loam mixtures to  $CO_2$  (Extended Data Fig. 2a).

After 30 days the experiment was terminated and the top centimeter of the microcosm was discarded before the samples were dissected into a fresh fraction and air-dried fraction. The former was used within two weeks of sampling, while the latter was dried for a minimum of seven days before further analysis.

### Additional analyses conducted on incubated samples

As an indicator of soil structural stability against hydrological forces, we use the size distribution of isolated, water-stable aggregates as an indicator. The size distribution can be represented by a singular parameter, mean weight diameter (MWD)<sup>66</sup>, which is defined and calculated (equation (1)) as the sum of the mean diameter of each aggregate fraction (Supplementary Section B) multiplied by the mass contribution of that fraction to the total recovered weight of the soil.

$$MWD = \sum_{i=1}^n x_i w_i \quad (1)$$

All samples were fractionated into four aggregate size classes<sup>67</sup>: large macroaggregates ( $>2$  mm), small macroaggregates (2–250  $\mu m$ ), large microaggregates (250–53  $\mu m$ ) and a silt and clay sized fraction ( $<53$   $\mu m$ ). Approximately 10 g of soil sample were loaded into a sieve tower automated to rise and fall by 1 cm for 130 cycles while submerged in deionized water.

In analyzing the subsoil materials, we measured three states: (1) dispersed samples of the excavated subsoil to give context for the innate particle size distribution of the soil material (dispersion via Na-Pyrophosphate shaken overnight), (2) the sieved, excavated subsoil before incubation and (3) the incubated subsoil samples. The prior two treatments were lightly wetted 30 minutes before the analysis to bring the soil to a hydrated state. Otherwise, to minimize the effect of a drying and wetting cycle in structure formation, samples from the incubation, including all amended mixtures, were analyzed fresh within 2 weeks of harvest ( $n = 4$ ).

Lastly, to assess the change in free mineral surface area, SSA was measured a second time (under the same parameters) using two incubated samples of each soil.

### Multifunctionality score calculation

We conducted a quantitative scoring to evaluate the relative multifunctional potential of our organic amendment combinations. Using an averaging approach<sup>68</sup>, we compute an aggregate metric of multifunctionality after estimating scores for the individual functions of increased soil fertility, pollutant-retention capacity and contribution to the accrual of stable organic carbon. Individual function scores were calculated from a series of measured variables chosen based on their relation to the desired soil function. Each variable dataset and function score were standardized to the proportion of the maximum value within that dataset. The increased soil fertility attributed to each organic amendment combination was calculated based on the increase in nitrogen content, the increase in cation exchange capacity and the increase in water content at field capacity. In turn, the pollutant-retention capacity was calculated based on the retention capacity for heavy metals, zinc and copper and organic pollutants, tetrabutryn and mecoprop. Lastly, contribution to the accrual of stable organic carbon was determined by multiplying the input of each type of carbon by the inverse of the hydrogen to organic carbon ratio, a common determinant for the degree of aromatization and soil carbon chemical persistence<sup>22,69,70</sup>. As no significant difference was detected between the capacity of amended substrates and the subsoil material in inducing larger water-stable aggregates as an indicator for structural stability and subsequent influence on infiltration this function was left out. All functions were weighted equally within the index.

### Statistical analyses

Version 2023.12.1.402 of RStudio<sup>71</sup> was used for data handling (via writexl, v.1.5.4 and readxl, v.1.4.5)<sup>72–75</sup>, statistical analyses (via car, v.3.1 and lmeans, v.2.30) and data visualizations (via ggplot2, v.3.5.2)<sup>76</sup>. All categorical factors were test via one-sided ANOVA after checking for homogeneity of variance and for normality within the residuals using Levenes test and Shapiro–Wilks tests, however final judgments were

made via visual aids such as bar plots and QQ plots. A Tukey post-hoc analysis was used in comparing the pollutant-retention potential of organic parent materials. Due to the large number of possible statistical combinations, orthogonal contrasting was used as an alternative post-hoc test in all other cases (Supplementary Section B). We did this to add strength to our analyses, testing only the statistical combinations supporting our research questions: significant changes in mixture properties per addition of organic amendments compared to the subsoil; significant changes in biochar-amended mixture properties compared to the municipal compost control; significant changes in biochar-amended mixture properties compared to the granulated activated carbon control; and significant differences seen between a singular biochar mixture compared to the related dual biochar mixtures. Detailed results regarding the degrees of freedom, *F*-values, *t*-ratios and *p*-values are available for the ANOVA, Tukey and contrasts in Supplementary Section B. The dataset supporting the results of this study are available on request from the corresponding author.

### Reporting summary

Further information on research design is available in the Nature Portfolio Reporting Summary linked to this article.

### Data availability

The data that support the findings of this study are available via figshare at <https://doi.org/10.6084/m9.figshare.30002656> (ref. 77).

### References

1. EU Soil Strategy for 2030 Reaping the Benefits of Healthy Soils for People, Food, Nature and Climate (European Commission, 2021); <https://eur-lex.europa.eu/legal-content/EN/TXT/PDF/?uri=CELEX:52021DC0699>
2. Morel, J. L., Chenu, C. & Lorenz, K. Ecosystem services provided by soils of urban, industrial, traffic, mining, and military areas (SUITMAS). *J. Soils Sediments* **15**, 1659–1666 (2015).
3. Huang, S.-L. & Hsu, W.-L. Materials flow analysis and emergy evaluation of Taipei's urban construction. *Landscape Urban Plann.* **63**, 61–74 (2003).
4. Minixhofer, P. et al. Towards the circular soil concept: optimization of engineered soils for green infrastructure application. *Sustainability* **14**, 905 (2022).
5. ENV\_WASGEN. Eurostat [https://doi.org/10.2908/ENV\\_WASGEN](https://doi.org/10.2908/ENV_WASGEN) (2024).
6. Rokia, S. et al. Modelling agronomic properties of Technosols constructed with urban wastes. *Waste Manag.* **34**, 2155–2162 (2014).
7. Cannavo, P., Guénon, R., Galopin, G. & Vidal-Beaudet, L. Technosols made with various urban wastes showed contrasted performance for tree development during a 3-year experiment. *Environ. Earth Sci.* **77**, 1–13 (2018).
8. Yilmaz, D. et al. Physical properties of structural soils containing waste materials to achieve urban greening. *J. Soils Sediments* **18**, 442–455 (2018).
9. Pruvost, C. et al. Tree growth and macrofauna colonization in technosols constructed from recycled urban wastes. *Ecol. Eng.* **153**, 105886 (2020).
10. Nehls, T., Rokia, S., Mekiffer, B., Schwartz, C. & Wessolek, G. Contribution of bricks to urban soil properties. *J. Soils Sediments* **13**, 575–584 (2013).
11. Knoll, S. et al. The potential of processed mineral construction and demolition waste to increase the water capacity of urban tree substrates—a pilot scale study in Munich. *Sustain. Cities Soc.* **113**, 105661 (2024).
12. Vidal-Beaudet, L., Rokia, S., Nehls, T. & Schwartz, C. Aggregation and availability of phosphorus in a Technosol constructed from urban wastes. *J. Soils Sediments* **18**, 456–466 (2018).
13. Deeb, M. et al. Interactive effects of compost, plants and earthworms on the aggregations of constructed technosols. *Geoderma* **305**, 305–313 (2017).
14. Malone, Z., Berhe, A. A. & Ryals, R. Impacts of organic matter amendments on urban soil carbon and soil quality: a meta-analysis. *J. Cleaner Prod.* **419**, 138148 (2023).
15. Joseph, S. et al. How biochar works, and when it doesn't: a review of mechanisms controlling soil and plant responses to biochar. *GCB Bioenergy* **13**, 1731–1764 (2021).
16. Zheng, X.-J. et al. Assessment of zeolite, biochar, and their combination for stabilization of multimetal-contaminated soil. *ACS Omega* **5**, 27374–27382 (2020).
17. Thompson, K. A. et al. Environmental comparison of biochar and activated carbon for tertiary wastewater treatment. *Environ. Sci. Technol.* **50**, 11253–11262 (2016).
18. Bayer, P., Heuer, E., Karl, U. & Finkel, M. Economical and ecological comparison of granular activated carbon (GAC) adsorber refill strategies. *Water Res.* **39**, 1719–1728 (2005).
19. Thengane, S. K. et al. Market prospects for biochar production and application in California. *Biofuels Bioprod. Biorefin.* **15**, 1802–1819 (2021).
20. Mohanty, S. K. et al. Plenty of room for carbon on the ground: potential applications of biochar for stormwater treatment. *Sci. Total Environ.* **625**, 1644–1658 (2018).
21. Rodriguez Mendez, Q., Fuss, S., Lück, S. & Creutzig, F. Assessing global urban CO<sub>2</sub> removal. *Nat. Cities* **1**, 413–423 (2024).
22. Lehmann, J. et al. Biochar in climate change mitigation. *Nat. Geosci.* **14**, 883–892 (2021).
23. Anlagen Zur Versickerung von Niederschlagswasser—Teil 1: Planung, Bau, Betrieb 95 (DWA, 2024); <https://de.dwa.de/de/regelwerk-news-volltext/arbeitsblatt-dwa-a-138-1-anlagen-zur-versickerung-von-niederschlagswasser-teil-1-planung-bau-betrieb.html>
24. Deeb, M. et al. Influence of organic matter content on hydro-structural properties of constructed technosols. *Pedosphere* **26**, 486–498 (2016).
25. Bucka, F. B., Pihlap, E., Kaiser, J., Baumgartl, T. & Kögel-Knabner, I. A small-scale test for rapid assessment of the soil development potential in post-mining soils. *Soil Tillage Res.* **211**, 105016 (2021).
26. Raciti, S. M. et al. Accumulation of carbon and nitrogen in residential soils with different land-use histories. *Ecosystems* **14**, 287–297 (2011).
27. O'Riordan, R., Davies, J., Stevens, C. & Quinton, J. N. The effects of sealing on urban soil carbon and nutrients. *SOIL* **7**, 661–675 (2011).
28. Wiesmeier, M. et al. Amount, distribution and driving factors of soil organic carbon and nitrogen in cropland and grassland soils of southeast Germany (Bavaria). *Agric. Ecosyst. Environ.* **176**, 39–52 (2013).
29. Morel, J. L., Schwartz, C., Florentin, L. & de Kimpe, C. in *Encyclopedia of Soils in the Environment* (ed. Hillel, D.) 202–208 (Elsevier, 2005); <https://doi.org/10.1016/B0-12-348530-4/00305-2>
30. Somerville, P. D., Farrell, C., May, P. B. & Livesley, S. J. Biochar and compost equally improve urban soil physical and biological properties and tree growth, with no added benefit in combination. *Sci. Total Environ.* **706**, 135736 (2020).
31. Kutlu, T., Guber, A. K., Rivers, M. L. & Kravchenko, A. N. Moisture absorption by plant residue in soil. *Geoderma* **316**, 47–55 (2018).
32. Maziarka, P. et al. Do you BET on routine? The reliability of N<sub>2</sub> physisorption for the quantitative assessment of biochar's surface area. *Chem. Eng. J.* **418**, 129234 (2021).
33. Guo, M., Song, W. & Tian, J. Biochar-facilitated soil remediation: mechanisms and efficacy variations. *Front. Environ. Sci.* **8**, 521512 (2020).



34. Yang, X. et al. Surface functional groups of carbon-based adsorbents and their roles in the removal of heavy metals from aqueous solutions: a critical review. *Chem. Eng. J.* **366**, 608–621 (2019).
35. Rabot, E., Wiesmeier, M., Schlüter, S. & Vogel, H.-J. Soil structure as an indicator of soil functions: a review. *Geoderma* **314**, 122–137 (2018).
36. Pronk, G. J., Heister, K., Ding, G.-C., Smalla, K. & Kögel-Knabner, I. Development of biogeochemical interfaces in an artificial soil incubation experiment; aggregation and formation of organo-mineral associations. *Geoderma* **189–190**, 585–594 (2012).
37. Yudina, A. & Kuzyakov, Y. Dual nature of soil structure: the unity of aggregates and pores. *Geoderma* **434**, 116478 (2023).
38. Dong, X., Guan, T., Li, G., Lin, Q. & Zhao, X. Long-term effects of biochar amount on the content and composition of organic matter in soil aggregates under field conditions. *J. Soils Sediments* **16**, 1481–1497 (2016).
39. Sun, F. & Lu, S. Biochars improve aggregate stability, water retention, and pore-space properties of clayey soil. *J. Plant Nutr. Soil Sci.* **177**, 26–33 (2014).
40. Wang, D., Fonte, S. J., Parikh, S. J., Six, J. & Scow, K. M. Biochar additions can enhance soil structure and the physical stabilization of C in aggregates. *Geoderma* **303**, 110–117 (2017).
41. Dai, H. et al. Water-stable aggregates and carbon accumulation in barren sandy soil depend on organic amendment method: a three-year field study. *J. Clean. Prod.* **212**, 393–400 (2019).
42. Zhou, H. et al. Biochar enhances soil hydraulic function but not soil aggregation in a sandy loam. *Eur. J. Soil Sci.* **70**, 291–300 (2019).
43. Awad, Y. M., Blagodatskaya, E., Ok, Y. S. & Kuzyakov, Y. Effects of polyacrylamide, biopolymer and biochar on the decomposition of <sup>14</sup>C-labelled maize residues and on their stabilization in soil aggregates. *Eur. J. Soil Sci.* **64**, 488–499 (2013).
44. Zhang, M. et al. Effects of straw and biochar amendments on aggregate stability, soil organic carbon, and enzyme activities in the Loess Plateau, China. *Environ. Sci. Pollut. Res.* **24**, 10108–10120 (2017).
45. Lehmann J. et al. in *Biochar for Environmental Management: Science, Technology and Implementation* 2nd edn (eds Lehmann, J. & Joseph, S.) Ch. 10 (Routledge, 2015).
46. Angst, G. et al. Unlocking complex soil systems as carbon sinks: multi-pool management as the key. *Nat. Commun.* **14**, 2967 (2023).
47. Amelung, W. et al. *Scheffer/Schachtschabel Lehrbuch Der Bodenkunde* (Springer-Verlag, 2018).
48. Rowley, M. C., Grand, S. & Verrecchia, ÉP. Calcium-mediated stabilisation of soil organic carbon. *Biogeochemistry* **137**, 27–49 (2018).
49. Fernández-Ugalde, O. et al. Effect of carbonates on the hierarchical model of aggregation in calcareous semi-arid Mediterranean soils. *Geoderma* **164**, 203–214 (2011).
50. Bucka, F. B., Felde, V. J. M. N. L., Peth, S. & Kögel-Knabner, I. Complementary effects of sorption and biochemical processing of dissolved organic matter for emerging structure formation controlled by soil texture. *J. Plant Nutr. Soil Sci.* **187**, 51–62 (2023).
51. Bauer, M., Thuro, K., Marcus, S. & Neumann, P. The geology of Munich (Germany) and its significance for ground modelling in urban areas. *Geotechnik* **28**, 454 (2005).
52. *Umgang Mit Bodenmaterial* (Bayerisches Landesamt für Umwelt, 2022).
53. Schielein, P. & Schellmann, G. Erläuterungen zur quartärgeologischen Karte 1:25.000 des Lech- und Schmuttertals auf Blatt 7531 Gersthofen – Kartierungsergebnisse aus dem Jahr 2011. *Bamberger Geogr. Schriften SF* **12**, 41–73 (2011).
54. Hobley, E. U., Murphy, B. & Simmons, A. Comment on ‘Soil organic stocks are systematically overestimated by misuse of the parameters bulk density and rock fragment content’ by Poeplau et al. (2017). *SOIL* **4**, 169–171 (2018).
55. Kaya, D. et al. Considerations for evaluating innovative stormwater treatment media for removal of dissolved contaminants of concern with focus on biochar. *Chemosphere* **307**, 135753 (2022).
56. Schaefer, J. & Stejskal, E. O. Carbon-13 nuclear magnetic resonance of polymers spinning at the magic angle. *J. Am. Chem. Soc.* **98**, 1031–1032 (1976).
57. Knicker, H. & Lüdemann, H.-D. N-15 and C-13 CPMAS and solution NMR studies of N-15 enriched plant material during 600 days of microbial degradation. *Org. Geochem.* **23**, 329–341 (1995).
58. Baldock, J. A. et al. Assessing the extent of decomposition of natural organic materials using solid-state <sup>13</sup>C NMR spectroscopy. *Soil Res.* **35**, 1061–1084 (1997).
59. Freitas, J. C. C., Bonagamba, T. J. & Emmerich, F. G. <sup>13</sup>C High-resolution solid-state NMR study of peat carbonization. *Energy Fuels* **13**, 53–59 (1999).
60. Spahr, S. et al. Performance of biochars for the elimination of trace organic contaminants and metals from urban stormwater. *Environ. Sci. Water Res. Technol.* **8**, 1287–1299 (2022).
61. Brunauer, S., Emmett, P. H. & Teller, E. Adsorption of Gases in Multimolecular Layers. *J. Am. Chem. Soc.* **60**, 309–319 (1938).
62. Bucka, F. B., Kölbl, A., Uteau, D., Peth, S. & Kögel-Knabner, I. Organic matter input determines structure development and aggregate formation in artificial soils. *Geoderma* **354**, 113881 (2019).
63. Lal, R. Soil organic matter and water retention. *Agron. J.* **112**, 3265–3277 (2020).
64. Bimüller, C. et al. Decoupled carbon and nitrogen mineralization in soil particle size fractions of a forest topsoil. *Soil Biol. Biochem.* **78**, 263–273 (2014).
65. Luxhøj, J., Bruun, S., Stenberg, B., Breland, T. A. & Jensen, L. S. Prediction of gross and net nitrogen mineralization-immobilization-turnover from respiration. *Soil Sci. Soc. Am. J.* **70**, 1121–1128 (2006).
66. Márquez, C. O., Garcia, V. J., Cambardella, C. A., Schultz, R. C. & Isenhardt, T. M. Aggregate-size stability distribution and soil stability. *Soil Sci. Soc. Am. J.* **68**, 725–735 (2004).
67. Tisdall, J. M. & Oades, J. M. Organic matter and water-stable aggregates in soils. *J. Soil Sci.* **33**, 141–163 (1982).
68. Byrnes, J. E. K. et al. Investigating the relationship between biodiversity and ecosystem multifunctionality: challenges and solutions. *Methods Ecol. Evol.* **5**, 111–124 (2014).
69. Janu, R. et al. Biochar surface functional groups as affected by biomass feedstock, biochar composition and pyrolysis temperature. *Carbon Resour. Convers.* **4**, 36–46 (2021).
70. Harvey, O. R. et al. An index-based approach to assessing recalcitrance and soil carbon sequestration potential of engineered black carbons (biochars). *Environ. Sci. Technol.* **46**, 1415–1421 (2012).
71. RStudio Team. *RStudio: Integrated Development for R* (RStudio, 2023).
72. Ooms, J. writexl: export data frames to Excel ‘xlsx’ format. R package v.1.5.0. CRAN <https://CRAN.R-project.org/package=writexl> (2025).
73. Bryan, J. & Wickham, H. readxl: read Excel files. R package v.1.4.3. CRAN <https://CRAN.R-project.org/package=readxl> (2023).
74. Fox, J. et al. Package ‘car’. *Vienna R Found. Stat. Comput.* **16**, 333 (2012).

75. Lenth, R. & Lenth, M. R. Package 'lsmeans'. *Am. Stat.* **34**, 216–221 (2018).
76. Wickham, H. *Ggplot2: Elegant Graphics for Data Analysis* (Springer-Verlag New York, 2016).
77. Porter, L., Bucka, F. B., Pérez-Curtidor, N., Egerer, M. & Kögel-Knabner, I. NATCITIES-24060685\_Dataset. *figshare* <https://doi.org/10.6084/m9.figshare.30002656> (2025).

## Acknowledgements

We acknowledge the financial support of the Deutsche Forschungsgemeinschaft (DFG) as a part of the project Urban Green Infrastructure (GRK 2679, I.K.-K., M.E.). We thank Sebastian Knoll and Andreas Thaler for guidance in choosing and providing subsoil material for the project; B. Helmreich and M. Deeb for insightful discussion on decentralized urban drainage systems and soil physics; J. Guigue and G. Villalba Ayala for their inputs on early drafts of the paper; J. Moosholzer for sharing his expertise on data visualization; and the student laboratory assistants S. Spinoso-Sosa, R. Rozsnyoi, K. Spriggs and Y. Huang.

## Author contributions

L.P. helped design the experiment, carried out the soil analyses and incubation, collected and analyzed the data and wrote the paper; F.B.B. and I.K.-K. designed and supervised the experiment and data analysis and contributed to editing the drafts; N.P.-C. conducted the pollutant immobilization analyses, helped with data analysis and editing the drafts; M.E. contributed to writing the paper, supervision of the data analysis and editing the drafts.

## Funding

Open access funding provided by Technische Universität München.

## Competing interests

The authors declare no competing interests.

## Additional information

**Extended data** is available for this paper at <https://doi.org/10.1038/s44284-025-00332-9>.

**Supplementary information** The online version contains supplementary material available at <https://doi.org/10.1038/s44284-025-00332-9>.

**Correspondence and requests for materials** should be addressed to Lauren Porter.

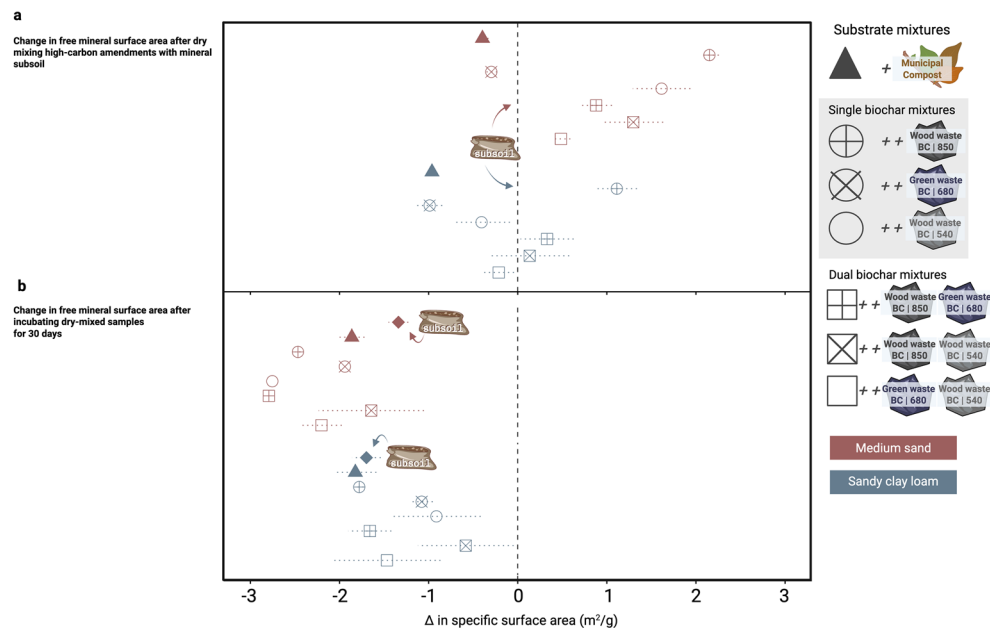
**Peer review information** *Nature Cities* thanks Geoffroy Séré and the other, anonymous, reviewer(s) for their contribution to the peer review of this work. Peer reviewer reports are available.

**Reprints and permissions information** is available at [www.nature.com/reprints](http://www.nature.com/reprints).

**Publisher's note** Springer Nature remains neutral with regard to jurisdictional claims in published maps and institutional affiliations.

**Open Access** This article is licensed under a Creative Commons Attribution 4.0 International License, which permits use, sharing, adaptation, distribution and reproduction in any medium or format, as long as you give appropriate credit to the original author(s) and the source, provide a link to the Creative Commons licence, and indicate if changes were made. The images or other third party material in this article are included in the article's Creative Commons licence, unless indicated otherwise in a credit line to the material. If material is not included in the article's Creative Commons licence and your intended use is not permitted by statutory regulation or exceeds the permitted use, you will need to obtain permission directly from the copyright holder. To view a copy of this licence, visit <http://creativecommons.org/licenses/by/4.0/>.

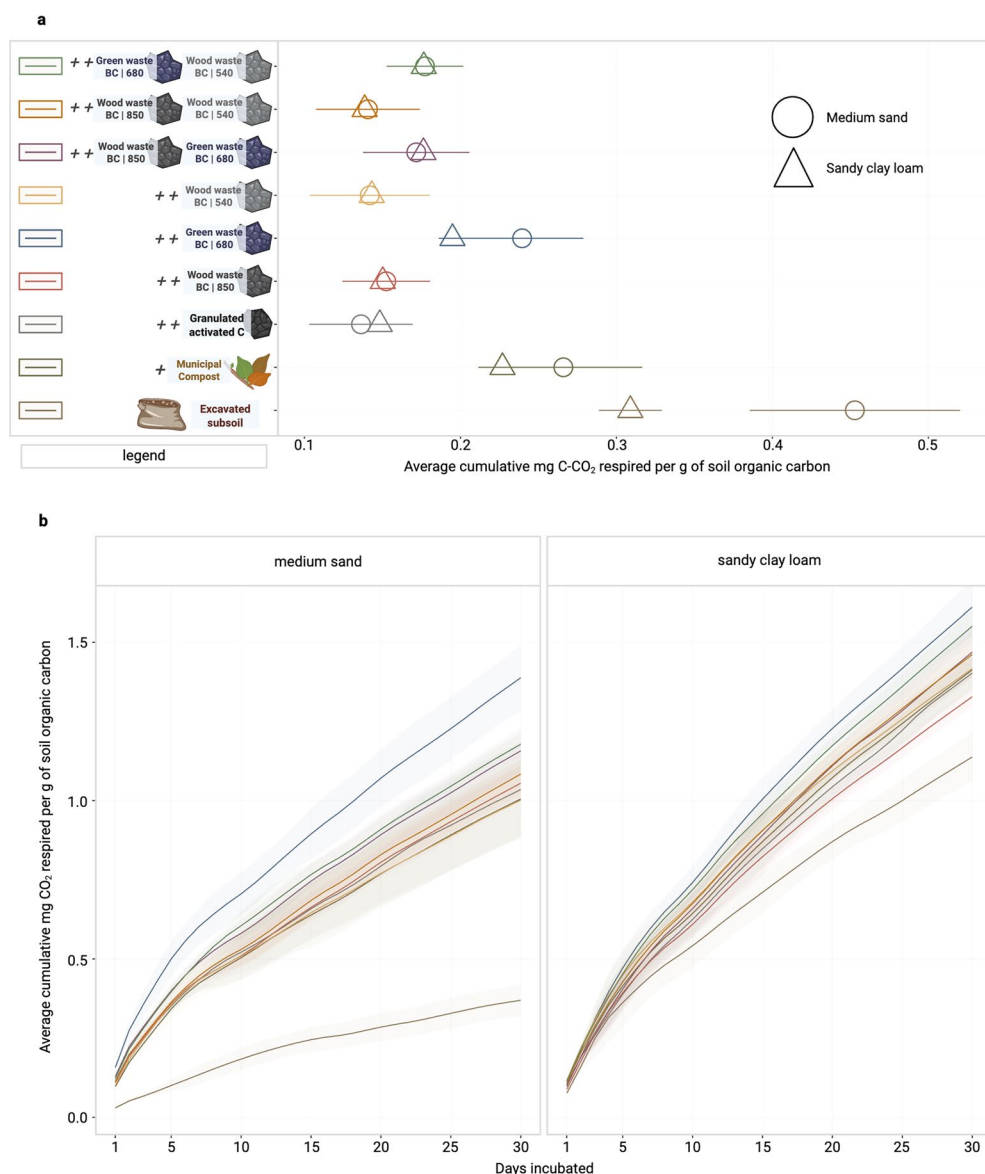
© The Author(s) 2025



**Extended Data Fig. 1 | Changes in specific surface areas (free mineral surface area) of the substrate mixtures.** The changes in specific surface area ( $n = 2$ ) associated with **a.** dry-mixing the amendments with the baseline mineral soils and **b.** changes in free mineral surface area after incubating dry-mixed samples

for 30 days. Benchmark mixture with granulated activated carbon (GAC) not included. See Fig. 1 for in depth mixture clarification. Figure created using [BioRender.com](https://BioRender.com).





**Extended Data Fig. 2 | Microbial respiration graphs. a.** The cumulative C-CO<sub>2</sub> (mg) respired across the 30 day incubation normalized to the substrate OC content (g) (n = 5). Points with error bars represent the mean  $\pm$  one standard deviation. **b.** The cumulation of CO<sub>2</sub> (mg) respired across the 30 day incubation

(n = 5). Lines with error ribbons represent the mean  $\pm$  one standard deviation. Abbreviations: XX | ### gives the waste type | pyrolysis temperature in °C.

The legend for the curves in part **b** can be found in part **a**. See Fig. 1 for in depth mixture clarification. Figure created using [BioRender.com](https://www.biorender.com).

## Extended Data Table 1 | Characteristics of parent materials

a

Characteristics	Augsburg soil	Munich soil
Location	Gersthofen 48.444, 10.858	Neufreiman 48.200, 11.600
<b>Excavated subsoil</b>		
Coarse elements > 2mm (%) <sup>†</sup>	8	64
Carbonate Content (%) (n=5)	50.5	0.5
<b>Active soil fraction</b>		
Clay (%) (n=2)	7	23
Sand (%) (n=2)	90	61
Soil Texture Classification	Medium Sand (MS)	Sandy Clay Loam (SCL)

b

Organic amendment	Compost (mGWC)	Wood waste BC   850 (WW   850)	Green waste BC   680 (GW   680)	Wood waste BC   540 (WW   540)	Granulated activated carbon (GAC)
Feedstock	Municipal green waste	Mixed forestry residues	Cocoa shells	Mixed forestry residues	Virgin coal
Pyrolysis (C%) <sup>†</sup>	-	850	680	540	830
OC (mg/g) (n=5)	260	760	575	790	870
IC (mg/g) (n=5)	15.4	7.3	1.9	1.3	-
N (mg/g) (n=5)	15.3	2.9	23.6	5.3	3.3
CN Ratio (n=5)	20	305	28	174	307
H/OC <sup>†</sup>	-	0.15	0.24	0.34	-
Ash (%) <sup>†</sup>	-	9.5	2.1	3.6	-
pH (H <sub>2</sub> O) (n=3)	8.07	9.9	10.7	8.2	-
Particles < 0.5mm (mg/g) (n=2)	473*	684 <sup>†</sup>	334 <sup>†</sup>	287 <sup>†</sup>	16*

a. description of the excavated mineral subsoil materials b. characteristics and parameters of the organic amendments. Means based on 5 replicates except where asterisks are indicated, \* indicates self-measured with 2 replicates while <sup>†</sup> indicates that data for this parameter was received from the parent company

Extended Data Table 2 | Pollutant removal by the two subsoil materials

Soil type	Heavy metal				Organic pollutants			
	Zinc		Copper		Mecoprop		Terabutryn	
	Av.	sd	Av.	sd	Av.	sd	Av.	sd
Medium sand	26.2 %	1.3%	54.3 %	3.9%	-3.3%	0.7%	3.1%	1.0%
Sandy clay loam	35.8 %	4.0%	68.6 %	5.1%	9.3%	1.9%	17.4%	5.1%

The average (av.) removal of pollutants (n=3) in percent of the original spiked dosage and the standard deviation for the Medium Sand (MS – Augsburg) and Sandy Clay Loam (SCL – Munich)



Extended Data Table 3 | Released Na, K, Mg, Ca and total sum of cations in cmol charge /kg

		Controls (CONs)		Single biochar mixtures (SBMs)			Dual biochar mixtures (DBMs)		
Substrate Mixtures	Excavated Subsoil	+ 4% mGWC	+ 2% MGWC + 2% GAC	+ 2% MGWC + 2% WW 850	+ 2% MGWC + 2% WW 540	+ 2% MGWC + 2% GW 680	+ 2% MGWC + 1% WW 850 + 1% GW 680	+ 2% MGWC + 1% WW 540 + 1% WW 680	+ 2% MGWC + 1% WW 850 + 1% WW 540
Ca									
SCL	4.75 ±0.89	8.54 ±1.61	6.23 ±0.73	6.63 ±0.82	6.52 ±0.47	6.59 ±0.88	6.12 ±0.48	5.82 ±1.11	6.33 ±0.61
MS	11.89 ±0.93	14.96 ±1.21	13.44 ±0.38	13.65 ±0.97	13.42 ±0.67	10.66 ±0.99	11.93 ±0.69	11.78 ±0.64	13.4 ±0.55
K									
SCL	0.79 ±0.2	1.25 ±0.07	0.9 ±0.1	1.22 ±0.06	1.22 ±0.11	4.45 ±0.47	2.67 ±0.23	2.59 ±0.3	1.22 ±0.12
MS	0.62 ±0.18	1.07 ±0.07	0.86 ±0.09	1.22 ±0.15	0.98 ±0.1	4.94 ±0.18	2.93 ±0.17	2.93 ±0.12	1.31 ±0.14
Mg									
SCL	0.85 ±0.1	1.6 ±0.44	1.3 ±0.31	1.23 ±0.19	1.12 ±0.2	1.52 ±0.43	1.26 ±0.15	1.23 ±0.21	1.12 ±0.08
MS	0.62 ±0.18	1.07 ±0.07	0.86 ±0.09	1.22 ±0.15	0.98 ±0.1	4.94 ±0.18	2.93 ±0.17	2.93 ±0.12	1.31 ±0.14
Na									
SCL	0.05 ±0.12	-0.01 ±0.01	-0.01 ±0.01	0 ±0.02	0 ±0.01	0.05 ±0.11	0 ±0.02	-0.02 ±0.01	0.01 ±0.03
MS	0.03 ±0.01	0.05 ±0.02	0.04 ±0	0.08 ±0.07	0.04 ±0.01	0.05 ±0.01	0.04 ±0.02	0.05 ±0.01	0.05 ±0.02
Total									
SCL	6.44 ±0.78	11.38 ±2.08	8.41 ±0.96	9.07 ±1.05	8.87 ±0.7	12.61 ±1.24	10.04 ±0.82	9.62 ±1.23	8.68 ±0.59
MS	14.49 ±1.35	18.37 ±1.6	13.08 ±7.33	17.03 ±1.28	16.35 ±0.75	17.73 ±1.26	17 ±0.95	16.78 ±0.86	16.78 ±0.77

Presented as the mean ± one standard deviation. Calcium estimates subject to carbonate release (n=5). Abbreviations MGWC – municipal compost, GAC – granulated activated carbon, WW|850 – high temperature wood-waste biochar, WW|540 - low temperature wood-waste biochar, GW|680 – green-waste biochar. SCL – sandy clay loam (Munich), MS – medium sand (Augsburg). Percentages refer to percent mass contribution of the amendments to the substrate mixture.

## Reporting Summary

Nature Portfolio wishes to improve the reproducibility of the work that we publish. This form provides structure for consistency and transparency in reporting. For further information on Nature Portfolio policies, see our [Editorial Policies](#) and the [Editorial Policy Checklist](#).

### Statistics

For all statistical analyses, confirm that the following items are present in the figure legend, table legend, main text, or Methods section.

n/a Confirmed

- |                                     |                                     |  |
|-------------------------------------|-------------------------------------|--|
| <input type="checkbox"/>            | <input checked="" type="checkbox"/> | The exact sample size ( $n$ ) for each experimental group/condition, given as a discrete number and unit of measurement  |
| <input type="checkbox"/>            | <input checked="" type="checkbox"/> | A statement on whether measurements were taken from distinct samples or whether the same sample was measured repeatedly  |
| <input type="checkbox"/>            | <input checked="" type="checkbox"/> | The statistical test(s) used AND whether they are one- or two-sided<br><i>Only common tests should be described solely by name; describe more complex techniques in the Methods section.</i>   |
| <input type="checkbox"/>            | <input checked="" type="checkbox"/> | A description of all covariates tested   |
| <input type="checkbox"/>            | <input checked="" type="checkbox"/> | A description of any assumptions or corrections, such as tests of normality and adjustment for multiple comparisons  |
| <input type="checkbox"/>            | <input checked="" type="checkbox"/> | A full description of the statistical parameters including central tendency (e.g. means) or other basic estimates (e.g. regression coefficient) AND variation (e.g. standard deviation) or associated estimates of uncertainty (e.g. confidence intervals) |
| <input type="checkbox"/>            | <input checked="" type="checkbox"/> | For null hypothesis testing, the test statistic (e.g. $F$ , $t$ , $r$ ) with confidence intervals, effect sizes, degrees of freedom and $P$ value noted<br><i>Give <math>P</math> values as exact values whenever suitable.</i>                            |
| <input checked="" type="checkbox"/> | <input type="checkbox"/>            | For Bayesian analysis, information on the choice of priors and Markov chain Monte Carlo settings   |
| <input checked="" type="checkbox"/> | <input type="checkbox"/>            | For hierarchical and complex designs, identification of the appropriate level for tests and full reporting of outcomes   |
| <input checked="" type="checkbox"/> | <input type="checkbox"/>            | Estimates of effect sizes (e.g. Cohen's $d$ , Pearson's $r$ ), indicating how they were calculated   |

Our web collection on [statistics for biologists](#) contains articles on many of the points above.

### Software and code

Policy information about [availability of computer code](#)

Data collection	No software was used to collect data.
Data analysis	Version 2023.12.1.402 of RStudio (RStudio Team 2023) was used for data handling (via writexl, v.1.5.4, Ooms 2020 & readxl, v.1.4.5, Bryan 2019), statistical analyses and data visualizations (via ggplot2, v.3.5.2, Wickham 2019). Biorender was used for post-statistical graphics editing.

For manuscripts utilizing custom algorithms or software that are central to the research but not yet described in published literature, software must be made available to editors and reviewers. We strongly encourage code deposition in a community repository (e.g. GitHub). See the Nature Portfolio [guidelines for submitting code & software](#) for further information.

### Data

Policy information about [availability of data](#)

All manuscripts must include a [data availability statement](#). This statement should provide the following information, where applicable:

- Accession codes, unique identifiers, or web links for publicly available datasets
- A description of any restrictions on data availability
- For clinical datasets or third party data, please ensure that the statement adheres to our [policy](#)

The data supporting the findings of this study are available on rFigshare, under the DOI: 10.6084/m9.figshare.30002656

## Human research participants

Policy information about [studies involving human research participants and Sex and Gender in Research](#).

Reporting on sex and gender

Population characteristics

Recruitment

Ethics oversight

Note that full information on the approval of the study protocol must also be provided in the manuscript.

## Field-specific reporting

Please select the one below that is the best fit for your research. If you are not sure, read the appropriate sections before making your selection.

☐ Life sciences

☐ Behavioural & social sciences

☒ Ecological, evolutionary & environmental sciences

For a reference copy of the document with all sections, see [nature.com/documents/nr-reporting-summary-flat.pdf](https://nature.com/documents/nr-reporting-summary-flat.pdf)

## Ecological, evolutionary & environmental sciences study design

All studies must disclose on these points even when the disclosure is negative.

Study description

We studied the effect of combinations of high-carbon organic amendments mixed with urban sediment waste material on a number of indicators for urban soil ecosystem services - namely fertility for urban greening, stormwater contaminant sorption and carbon accrual. After a 30-day incubation experiment, we further investigated the development of soil structure, a strong supporting factor in our selected three ecosystem services.

We used a full factorial design, with five experimental units (microcosms) for each treatment (soil material x high-carbon organic amendment combination). Soil material as a factors contained two-levels, sourced as waste subsoils from construction sites in the cities of Munich and Augsburg, while there were nine levels of high-carbon organic amendment combinations - (i) no organic addition, (ii) addition of 4% municipal compost, (iii) addition of 2% municipal compost and 2% granulated activated carbon, (iv-vi) addition of singular biochars all contain 2% municipal compost as well as iv) 2% biochar of woody waste produced at 850°C (WW|850) v) 2% biochar of green-waste produced at 680°C (GW|680) & vi) 2% biochar of woody waste produced at 540°C (WW|540), and the dual biochar mixtures (vii - ix) containing combinations of the three biochars at 1% (percentages indicate mass contribution of high carbon organic amendments to the mineral-organic mixtures). For a total of 90 experimental units. Statistical comparisons were only made directly between organic amendments.

The soil properties and processes evaluated included adsorption capacity, carbon chemical composition, bulk density, water holding capacity, pH, cation exchange capacity, total nitrogen, organic carbon, inorganic carbon, specific surface area, microbial respiration, aggregate size distribution and mean weight diameter.

Research sample

The soil material used in this study are two "destined-to-be-waste" subsoils obtained from construction companies. They represent how a recycled waste material can be used in a local, circular economy. The two cities chosen, Munich and Augsburg, are two of the most populated cities in the southeastern German state of Bavaria.

Sampling strategy

Subsoil material was collected in large quantities (20 - 50 kg) from heaps of excavated, discarded construction waste and brought back to the lab to be air-dried, sieved to 2mm and homogenized.

After incubation, sampling of the microcosms included removing an approximate 1cm top and bottom layer of the microcosm soil to reduce edge effects.

Data collection

Natalie Pérez-Curtidor conducted the adsorption batch experiments of the high-carbon organic amendments.

Lauren Porter carried out the incubation and all measurements on the mineral soil and mixtures.

Timing and spatial scale

The Munich subsoil was acquired in October 2022, while the Augsburg subsoil was obtained in January 2023. The batch adsorption experiments with the high-carbon organic amendments were conducted in December 2022. The incubations were conducted between January and April of 2023 and all mineral material and mixture analyses were conducted between January 2023 and March 2024.

Data exclusions

Due to a microcosm malfunction, one microcosm replicate (Munich soil material, + 2% m/m granulated activated carbon) was destroyed during the incubation and therefore was excluded from all following-up analyses.

Reproducibility

Our incubation protocol was based off of previous experiments, the works of Bucka et al. 2019, 2021a and 2021b (one of the co-authors), which were conducted on similar artificial and constructed soils.

Randomization

Four suction plates were used to incubate the microcosms. Each plate contained at least one of each treatment to diminish the impact of plates on the overall results, within each plate the position of the microcosms on the plate were randomized.

Blinding

Blinding did not apply to this study.

Did the study involve field work?

☒ Yes ☐ No

## Field work, collection and transport

Field conditions

The Munich excavated subsoil material was collected in October 2022 (~7°C, light rainfall), while the Augsburg excavated subsoil material was collected in January 2023 (~2°C, no rainfall). Both were collected from heaps of excavated soil material already removed by the construction companies.

The thermal chamber was kept dark (except while working in the chamber) at a constant temperature of 20°C.

Location

The Munich soil was sampled from the up-and-coming neighborhood of Neufreiman (48.200, 11.600), while the Augsburg soil was sampled from the neighborhood of Gersthofen (48.444, 10.858).  
Analyses took place at the Technical University of Munich Garching and Weihenstephan Campuses

Access &amp; import/export

All samples were collected after permission was given by respective companies and contacts who owned the subsoil waste.

Disturbance

Disturbance does not apply to this study.

## Reporting for specific materials, systems and methods

We require information from authors about some types of materials, experimental systems and methods used in many studies. Here, indicate whether each material, system or method listed is relevant to your study. If you are not sure if a list item applies to your research, read the appropriate section before selecting a response.

### Materials & experimental systems

n/a	Involved in the study
<input checked="" type="checkbox"/>	<input type="checkbox"/> Antibodies
<input checked="" type="checkbox"/>	<input type="checkbox"/> Eukaryotic cell lines
<input checked="" type="checkbox"/>	<input type="checkbox"/> Palaeontology and archaeology
<input checked="" type="checkbox"/>	<input type="checkbox"/> Animals and other organisms
<input checked="" type="checkbox"/>	<input type="checkbox"/> Clinical data
<input checked="" type="checkbox"/>	<input type="checkbox"/> Dual use research of concern

### Methods

n/a	Involved in the study
<input checked="" type="checkbox"/>	<input type="checkbox"/> ChIP-seq
<input checked="" type="checkbox"/>	<input type="checkbox"/> Flow cytometry
<input checked="" type="checkbox"/>	<input type="checkbox"/> MRI-based neuroimaging